

AD-A083 334

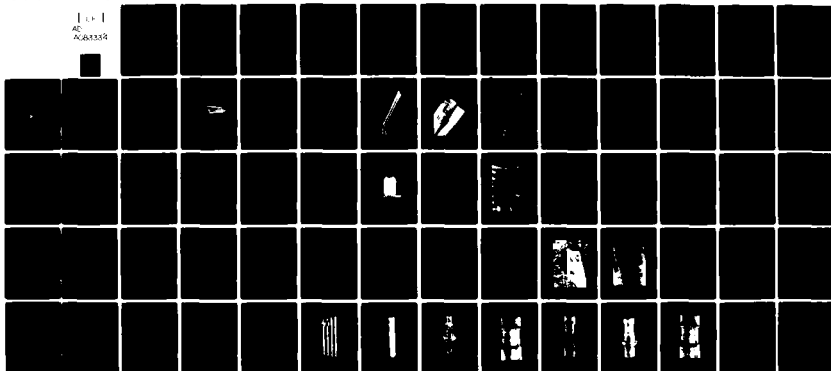
SRI INTERNATIONAL MENLO PARK CA F/B 20/11
SOURCE PRESSURE AND FLOW SAMPLE MEASUREMENTS ON DABS TESTS S2 A--ETC(U)
JAN 79 D D KEOUGH, L B HALL, R W GATES DNA001-77-C-0219

DNA-4943F

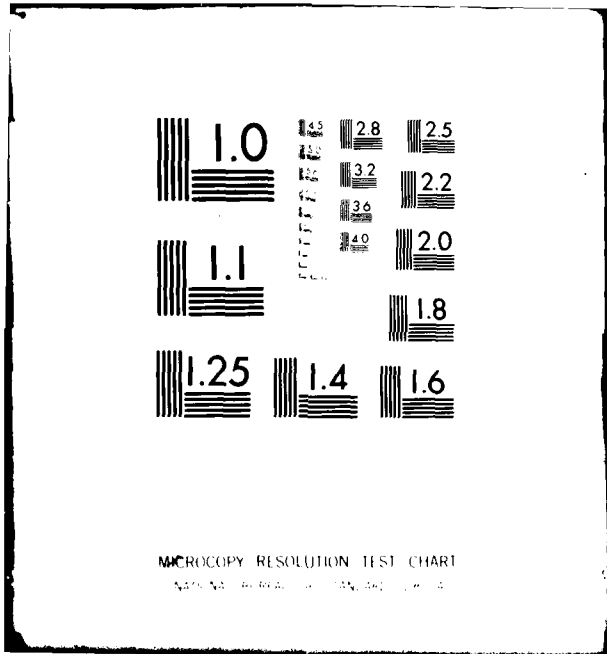
NL

UNCLASSIFIED

1-1
AD
ADDRESS



END
DATE
FILMED
5-80
DTIC



MICROCOPY RESOLUTION TEST CHART
NATIONAL BUREAU OF STANDARDS-1963-A

(12) LEVEL III
nu

AD-E 300 728

DNA 4943F

ADA 083334

SOURCE PRESSURE AND FLOW SAMPLE MEASUREMENTS ON DABS TESTS S2 AND S3

D. D. Keough
L. B. Hall
R. W. Gates
SRI International
333 Ravenswood Avenue
Menlo Park, California 94025

1 January 1979

Final Report for Period 14 April 1977—30 June 1978

CONTRACT No. DNA 001-77-C-0219

APPROVED FOR PUBLIC RELEASE;
DISTRIBUTION UNLIMITED.

S DTIC ELECTE D
APR 23 1980
B

THIS WORK SPONSORED BY THE DEFENSE NUCLEAR AGENCY
UNDER RDT&E RMSS CODE B344077462 H11CAXSX35506 H2590D.

DC FILE COPY

Prepared for
Director
DEFENSE NUCLEAR AGENCY
Washington, D. C. 20305

80 3 20 019

Destroy this report when it is no longer
needed. Do not return to sender.

PLEASE NOTIFY THE DEFENSE NUCLEAR AGENCY,
ATTN: STTI, WASHINGTON, D.C. 20305, IF
YOUR ADDRESS IS INCORRECT, IF YOU WISH TO
BE DELETED FROM THE DISTRIBUTION LIST, OR
IF THE ADDRESSEE IS NO LONGER EMPLOYED BY
YOUR ORGANIZATION.



UNCLASSIFIED

SECURITY CLASSIFICATION OF THIS PAGE (When Data Entered)

REPORT DOCUMENTATION PAGE		READ INSTRUCTIONS BEFORE COMPLETING FORM
1. REPORT NUMBER DNA 4943F	2. GOVT ACCESSION NO. AD-A083 334	3. RECIPIENT'S CATALOG NUMBER
4. TITLE (and Subtitle) SOURCE PRESSURE AND FLOW SAMPLE MEASUREMENTS ON DABS TESTS S2 AND S3	5. TYPE OF REPORT & PERIOD COVERED Final Report for Period 14 Apr 77—30 Jun 78	
	6. PERFORMING ORG. REPORT NUMBER SRI Project PYU-6334	
7. AUTHOR(s) D. D. Keough L. B. Hall R. W. Gates	8. CONTRACT OR GRANT NUMBER(s) DNA 001-77-C-0219 <i>new</i>	
	10. PROGRAM ELEMENT PROJECT, TASK AREA & WORK UNIT NUMBERS NWET Subtask H11CAXSX355-06	
9. PERFORMING ORGANIZATION NAME AND ADDRESS SRI International 333 Ravenswood Avenue Menlo Park, California 94025	11. CONTROLLING OFFICE NAME AND ADDRESS Director Defense Nuclear Agency Washington, D.C. 20305	
	12. REPORT DATE 1 January 1979	
14. MONITORING AGENCY NAME & ADDRESS (if different from Controlling Office)	13. NUMBER OF PAGES 68	
	15. SECURITY CLASS (of this report) UNCLASSIFIED	
15a. DECLASSIFICATION DOWNGRADING SCHEDULE		
16. DISTRIBUTION STATEMENT (of this Report) Approved for public release; distribution unlimited.		
17. DISTRIBUTION STATEMENT (of the abstract entered in Block 20, if different from Report)		
18. SUPPLEMENTARY NOTES This work sponsored by the Defense Nuclear Agency under RDT&E RMSS Code B344077462 H11CAXSX35506 H2590D.		
19. KEY WORDS (Continue on reverse side if necessary and identify by block number)		
Shock Pressures Pressure Gages Particulate Concentration Flow Samplers Piezoresistance DABS Shock Tube Ytterbium		
20. ABSTRACT (Continue on reverse side if necessary and identify by block number) Air shock pressure-time histories were measured in the HE source region of the Air Force Weapons Laboratory (AFWL) DABS S2 test to determine source characteristics. Steel-ytterbium flatpack gages previously used for the measurement of soil stress were modified, and static, uniaxial strain calibration was performed at pressures to 8 MPa. Results of static calibration at these low pressures and low strain rates agreed well with values extrapolated from high stress (500 MPa) uniaxial strain, shock data, indicating no		

DD FORM 1 JAN 73 1473

EDITION OF 1 NOV 65 IS OBSOLETE

UNCLASSIFIED

SECURITY CLASSIFICATION OF THIS PAGE (When Data Entered)

UNCLASSIFIED

SECURITY CLASSIFICATION OF THIS PAGE (When Data Entered)

20. ABSTRACT (Continued)

strain rate effects in the ytterbium piezoresistance sensor and definable response if the tensor state of strain is carefully controlled. The gages survived the environment in the DABS test within 3 m of the HE source and indicated a double shock structure with peak pressures of up to 98 MPa, possible slight prepressurization of the source chamber by the primacord initiation system, < 5% skewing of the air shock, and slightly higher pressures along the tube axis.

Postshot measurement of the gage resistance showed that, for gages in which gross damage did not occur, the pre- and postshot values agreed within a few percent, indicating no gage hysteresis.

Flow samplers consisting of steel tubes explosively closed at the ends during shock flow were fielded at two stations, 19 and 26 m on DABS S3 to determine the particulate matter concentration and for comparison of particulate matter arrival time with previously observed pressure variations. An existing design was modified to reduce metal fragments and use at considerably higher pressures. Four samplers were fielded in the DABS S3 test. Three of the downstream sampler ends functioned; one downstream and all four upstream ends failed to close. Although the samplers and mounting stands appeared to have survived undamaged, postshot examination of the samplers indicated that the severe flexing of the mounting baseplate and sampler tubes dislodged part of the explosive firing train. Comparison of particulates between the closed samplers and one completely open sampler indicated that particulates ranging from ~0.01 to ~0.05 cm diameter, were carried in the flow. However, it was not possible from these measurements to determine the contribution of these particulates to observed pressure-time waveforms in these regions or to the observed damage to structures.

UNCLASSIFIED

SECURITY CLASSIFICATION OF THIS PAGE (When Data Entered)

PREFACE

This work was sponsored by the Defense Nuclear Agency (DNA) under contract DNA 001-77-C-0219, Program Element NWET 62710H, Project H11CAXS, Task Area X355, Work Unit 06. Tom Kennedy of DNA served as the Contracting Officer.

The work was performed in conjunction with the Air Force Weapons Laboratory (AFWL) of Kirtland Air Force Base. Captain Ray, Joe Renick, and Joe Ayalla are thanked for their aid in constructing and fielding portions of the instrumentation and for assistance in providing preshot predictions.

Contributors at SRI were Paul De Carli, Dexter Witherly, and Al Bartlett.

ACCESSION for		
NTIS	White Section	<input checked="" type="checkbox"/>
DDC	Buff Section	<input type="checkbox"/>
UNANNOUNCED		<input type="checkbox"/>
JUSTIFICATION		
BY		
DISTRIBUTION/AVAILABILITY CODES		
Dist.	AVAIL.	and/or SPECIAL
A		-

CONTENTS

PREFACE	1
LIST OF ILLUSTRATIONS.	3
LIST OF TABLES	4
1. INTRODUCTION	5
2. BACKGROUND	6
Pressure Gages	6
Flatpack Gage	8
Flow Samplers.	10
3. MODIFICATIONS FOR DABS MEASUREMENTS	14
Pressure Gages	14
Flow Samplers.	25
4. DABS RESULTS	34
DABS, S2, Source Pressure.	34
DABS, S3, Flow Samplers.	45
REFERENCES	52
APPENDIX CLOSURE FAILURE ANALYSIS	55

ILLUSTRATIONS

<u>Figure</u>		<u>Page</u>
1	Basic Flatpack Configuration	9
2	Explosively Closed Flow Samplers	11
3	Flow Sampler Assembly (Reference 8)	12
4	Ytterbium-Steel Gage Assembly, Cover Plate Removed. .	15
5	Grid Location, Ytterbium-Steel Gage.	16
6	Completed Gage Assembly	17
7	Ytterbium-Steel Gage, Load-Unload Static Response. .	22
8	Timing and Recording System for Pressure Gages, DABS S2	24
9	DABS Flow Sampler	26
10	HE Closure Ring	28
11	Cross Sectional View of Explosively Closed Sampler Tube	29
12	Flow Samplers, Showing "A" Frame Stand	31
13	Plan View of Sampler Locations in DABS S3	32
14	Timing and Firing Circuits for Flow Samplers, DABS S3	33
15	Plan View of Pressure Gage Layout, DABS S2	35
16	Pressure-Time Profiles, DABS S2.	36
17	Flow Samplers (1 and 2), Postshot, Station 19-m, Showing Rear Closure (Pinched Portion) and Apparently Undamaged Stand	46
18	Flow Samplers (3 and 4), Postshot, Station 26-m, Showing One Rear Closure	47

<u>Figure</u>		<u>Page</u>
19	Particle Size Distribution of Flow Samples, 1, 2, 3, 4, and Control	48
20	Particle Size Distribution of Flow Samples 3 and 4.	50
A.1	Sampler Tubes, Postshot	57
A.2	Sampler Tube 3, 2 ^o -4 ^o Bend	58
A.3	Sampler Tube 1, Nose Cone Moved, HE Ring Compressed Axially	59
A.4	Sampler Tube 2, Front Mounting Clamp Moved Forward	60
A.5	Sampler Tube 2, Rear Mounting Clamp Moved Forward	61
A.6	Sampler Tube 4, Back Closure Ring	62
A.7	Sampler Tube 2, Axial Compression	63

TABLES

<u>Table</u>		<u>Page</u>
1	Summary of Gage Data, Shot S2	42
2	Comparison of Pre- and Postshot Gage Resistances.	44
A.1	Sampler Failure Evidence	56

1. INTRODUCTION

As part of the validation phase of the M-X program, the Air Force Weapons Laboratory (AFWL) conducted a series of shock tube tests on MX structures using a dynamic air blast simulator (DABS) at the Yuma Test Site, Yuma, Arizona. In these tests, an air shock was driven over a test bed by a planar explosive source. Peak pressures and pressure durations simulated those expected from a surface burst nuclear source. Part of the diagnostics of the planar HE source and of the flow in the shock tube required measurement of source pressure-time histories and measurement of the contribution of particulate matter to the damage experienced by M-X structures located downstream in the test bed. Under contract DNA 001-77-C-0219, SRI International provided support to the AFWL by designing, testing, and fielding instrumentation to perform these measurements. Pressure-time measurements were made on DABS, S2 and particulate samplers were fielded on DABS, S3.

The scope of the instrumentation development was confined to adapting existing techniques to function in the extreme ranges expected in the DABS tests. For the source measurements, a piezoresistance gage, formerly used for the measurement of high stresses in soils, was modified to function at considerably lower pressures. For sampling of particulate matter, explosively closed flow samplers were modified to function at pressures considerably higher than in past work by extending their range of operation from ≈ 2 to ≈ 7 MPa. This report describes the previous status of the instruments, the modifications made, preshot tests, the DABS field configuration, and the results. An analysis of the failure of portions of the flow sampler is also given.

2. BACKGROUND

Pressure Gages

The objective of measuring the pressure-time histories in the DABS source region was to provide data for comparison with calculations of the close-in, high pressure air shock produced by an array of individual explosive charges. The ability to calculate this region correctly aids in selecting configurations that will produce specific downstream loading of test structures. Of particular interest were the scalar and vectorial variations in the air shock and also the relative arrival times of the air shock and detonation gases. Knowledge of these parameters and development of techniques to measure them were to be used in designing and testing other arrays. In addition it was expected that a comparison of waveforms in this high pressure region with those obtained downstream at lower pressures would help to determine the source of a second pressure pulse observed in the latter region on previous DABS tests. The source of this pulse was postulated as either the detonation gases or particulate matter entrained in the flow.

Preshot calculations indicated that pressures might range from ten to several hundreds of megapascals and would, therefore, be beyond the range of conventional air shock instrumentation. To achieve the wide range required in measuring source pressures, we modified a standard, high pressure shock transducer (the steel flatpack gage) conventionally used for measuring stresses in soils. The modification consisted of repackaging and calibrating at the lower pressures. Details of the modification are discussed in Section 3.

Of particular concern in adapting the ytterbium-steel flatpack to the low pressure, long duration measurements were the sensitivity of the piezoresistance coefficient to the tensor state-of-strain and also to strain rate. These aspects of the response of a piezoresistance

sensor were considered as possibly detrimental in this application, but were offset by; 1) the prospect of low electrical noise levels of a low impedance sensor in an environment of high EM signals, and 2) the fast response, and the mechanical ruggedness of piezoresistance gages. To identify design requirements, we first reviewed the current status of ytterbium gages. This review is summarized below.

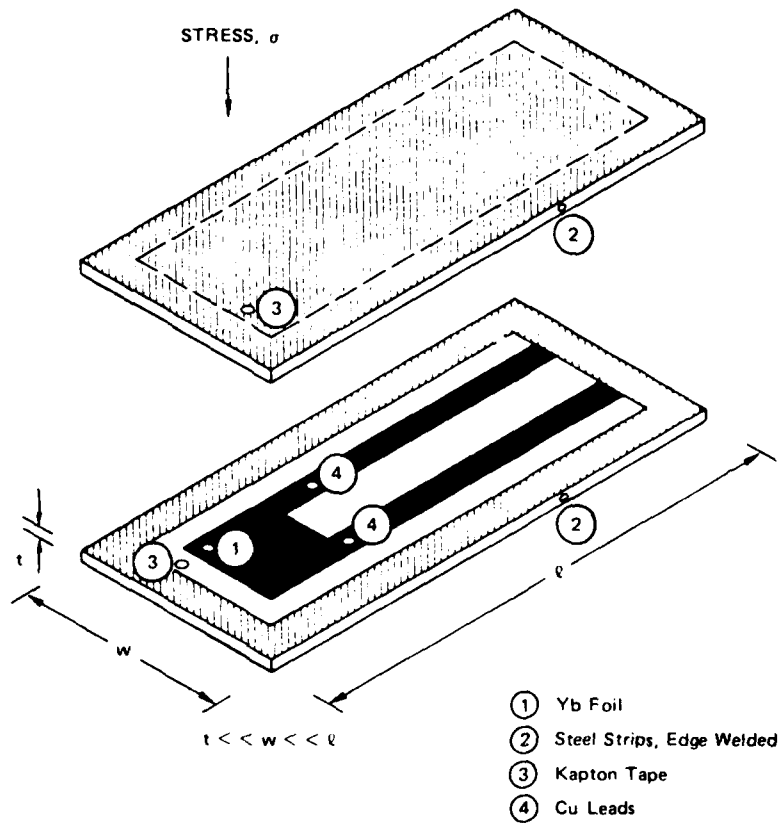
Smith et al.¹ showed that at low stresses, piezoresistance gages can indicate apparent negative stress and postulated the source as bending (tensile) strains in the sensor package. Ginsberg et al.² quantified the tensile response in uniaxial stress and found an initially negative change in resistance (ytterbium exhibits a positive change in compression) to a maximum of $\approx -2\%$. Upon further tensile strain, the resistance change became positive. These data are a manifestation of the sensitivity of piezoresistance sensors to the tensor state of strain; that is, the gage output, a scalar quantity, is not uniquely related to one component of the stress tensor. These tensile experiments² were performed at strain rates of the order of 10^1S^{-1} , whereas the compression response was determined under uniaxial strain at rates of the order of 10^5S^{-1} . Since loading in dynamic soil and air shocks is generally at intermediate rates, it is necessary to determine rate effects as well as tensor strain sensitivity. De Carli² performed static stress, low strain rate, calibration of gages consisting of ytterbium in an epoxy-fiberglass matrix and ytterbium stressed between plastic (PMMA) plattens. These results and other calibrations were reviewed by Keough.³ The conclusion was that in compression, either shock loaded (in uniaxial strain) or static, in which the strain state was not well defined, variations of $\pm 15\%$ in resistance existed at a given applied stress. This variation increased to 50% or more if large strains were coupled to the ytterbium by plastic flow of the encapsulant. In the work reported in reference 2, such strains were introduced at $\approx 80 \text{ MPa}$ by yielding of the PMMA plattens.

Hydrostatic compression data⁴ show a response of ytterbium higher than the uniaxial strain at stresses (pressures) below ≈ 500 MPa and lower at higher levels. Ginsberg et al. attempted to relate the two coefficients obtained from the two loading conditions by analyzing the piezoresistance strain tensor, using residual resistance data obtained from a measurement of hysteresis. The residual resistance was used to define the change due to mechanical yielding of the ytterbium. However, as pointed out by Gupta and Keough,⁵ the tests from which these data were obtained did not represent a strain-free state in the sensor after stress cycling; that is, release to zero compressive stress in a uniaxial strain shock experiment does not require all principal stresses to be zero.

In view of the uncertainties and possible ambiguities that might result in the reduction of resistance-time data to pressure-time data, it was decided to restrict the strain state in the sensor of the DABS gages to as close to uniaxial as possible by the gage configuration and then perform a few static calibration tests to evaluate the adequacy of the design. The static tests could also be compared with shock results to determine possible rate effects. The results of these tests are described in Section 3.

Flatpack Gage

The general construction of the flatpack gage is shown in Figure 1. This configuration was originally designed to prevent gage failure under compression loading due to loss of electrical leads by shorting through shearing or loss of continuity by failure at sensor-cable joints.⁶ To prevent failure, all elements of the gage (sensor, leads, insulator, and outer casing) were constructed with a high aspect ratio; i.e., the thickness (in the shock direction) was typically less than 1/20th of the width (in the plane of the shock). With this configuration, particle velocity equilibrium in all elements of the gage is achieved by more or less uniaxial strain deformation (in the σ direction of Figure 1). The high aspect ratio is maintained in the



MA-314522-88A

FIGURE 1 BASIC FLATPACK CONFIGURATION

lead portion of the gage in regions where the stresses are expected to be high and is used to form a transition to spatially separated regions where the stress is low enough to allow the use of conventional cables.

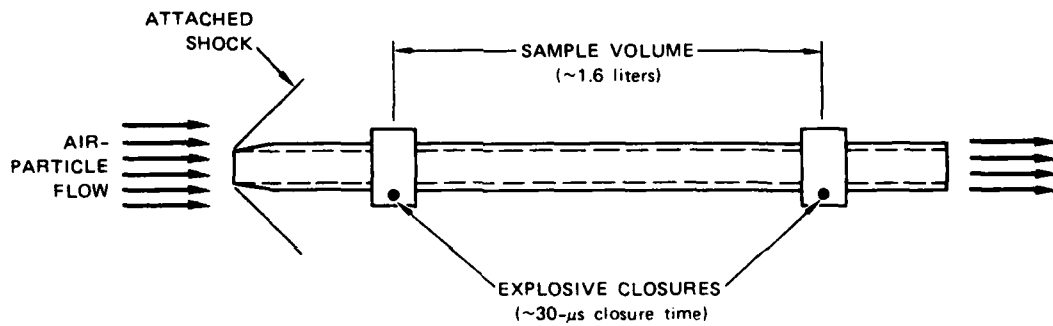
During later development of this gage,⁷ it became apparent that materials of high modulus and low Poisson's ratio were required for the gages' outer casing to minimize lateral strains in the piezo-resistance sensor. In the early stages of development, gage casings were constructed of Al_2O_3 , but proved unsatisfactory because of fracture during loading. Steel was substituted and proved satisfactory for measuring high stresses (2 GPa) in soil without failure. Recovery experiments with steel and with aluminum casings shocked to ~ 2 GPa showed that a larger lateral deformation occurred in the aluminum and caused gage failure. The casing mechanical properties as well as geometry were therefore an integral part of gage design.

The essential conclusions from prior work on the flatpack gage pertinent to the DABS measurements were therefore:

- A design having a high aspect ratio should survive the DABS environment.
- Steel strips should be used for the gage casing.
- The gage must be constructed to assure a known strain in the sensor.
- The final gage package should be calibrated at low pressures and low strain rates.
- Tensile strains must be minimized.

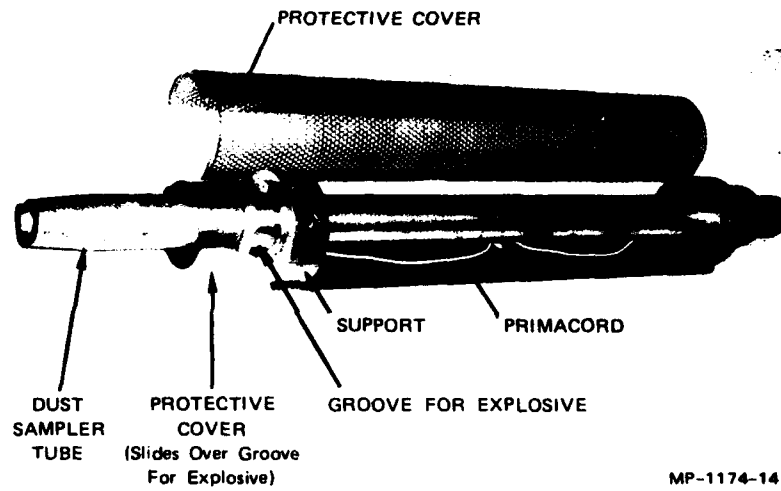
Flow Samplers

The particle flow samplers proposed for the DABS shock tube are based on the concept that a volume of the flow (~ 1.6 liters) is trapped in a cylindrical tube by simultaneous closure of both ends of the cylinder, as shown schematically in Figure 2 and pictorially in Figure 3. The concept is an adaptation of a tube closure system used by Lockheed Aircraft Corporation. Modifications for supersonic flow are described by Witherly.⁸ Critical to trapping of particulate matter in the flow are the aerodynamics of the flow at the upstream



MA-6334-12

FIGURE 2 EXPLOSIVELY CLOSED FLOW SAMPLER



MP-1174-14

FIGURE 3 FLOW SAMPLER ASSEMBLY, REFERENCE 8

opening and in the tube. The leading edge must be designed to assure that an attached shock is formed close enough to the tube that the particle trajectory is undisturbed until the particles enter the tube. This allows sampling of the "free stream" particulate matter. It is also necessary to reestablish velocity equilibrium between the gas and particles in the region between closures to prevent changes in concentration of the samples. Design parameters to meet these criteria had been determined from an analysis of gages developed to measure dust momentum flux.⁹ In the referenced work the closely attached shock was controlled by tapering the leading edge of the cylinder. Velocity equilibrium was found to be reestablished within three tube diameters.

Simultaneous closure of the ends of the cylinder is accomplished by collapsing a section of each end of the tube by circumferentially wrapped sheet explosive. Closure time is short compared with the flow transit time between explosive charges. For a 5-cm-O.D. tube, this time is approximately 30 μ s. The minimum dust concentration obtainable with this system is about 1 mg/cm³. Branched primacord, as shown in Figure 3, is used to initiate both closures from a single source. Specific features of the mounting hardware and explosive closure assemblies for samplers used in prior work are described by Witherly.⁹ The primary effort in the present program was to modify the existing design for use at the higher pressures and higher Mach numbers expected in the DABS shock tube. These modifications and the test results are described in the following sections.

3. MODIFICATIONS FOR DABS MEASUREMENTS

Pressure Gages

The flatpack gage constructed for the DABS S2 event is shown in Figures 4, 5, and 6. The gage consists of a 20- Ω , ytterbium grid of 5 x 7.5 cm and etched from 0.005-cm-thick foil.* This material with a known metallurgical history has been characterized by Ginsberg.² Electrical leads 0.005 cm thick by 0.635 cm wide were spot welded to the ytterbium before etching of the grid. This sensor assembly was then bonded to a layer of Kapton[†] adhesive tape, 0.005 cm thick and 5 cm wide. This tape was bonded to a thick steel backing plate (0.635 cm thick, 10 cm wide and 122 cm long) as shown in Figures 4 and 5. Details of the grid area are shown in Figure 5. Particular care was taken assembling the insulating tape layers (two on each steel strip) to assure bubble free bonding. This was accomplished by rolling out trapped air. A 0.16-cm-thick by 7.5-cm-wide cover plate (shown in Figure 5) was welded to the thick backing plate to form a completed gage assembly, as shown in Figure 6.

The cover and backing plates performed several functions. The cover acted as a diaphragm in contact with the foil-Kapton sensor. Its thickness and lateral dimensions were chosen so that its deflection at all pressures of interest was greater than the composite change in the thickness of the interior gage components, i.e.,

$$(\Delta t_c)_p < \delta_p \quad (1)$$

where t is the total thickness of the composite, δ is the deflection,

* Foil obtained from Research Chemicals, Inc., Phoenix, Arizona.

[†] Du Pont trademark for polyimide plastic.

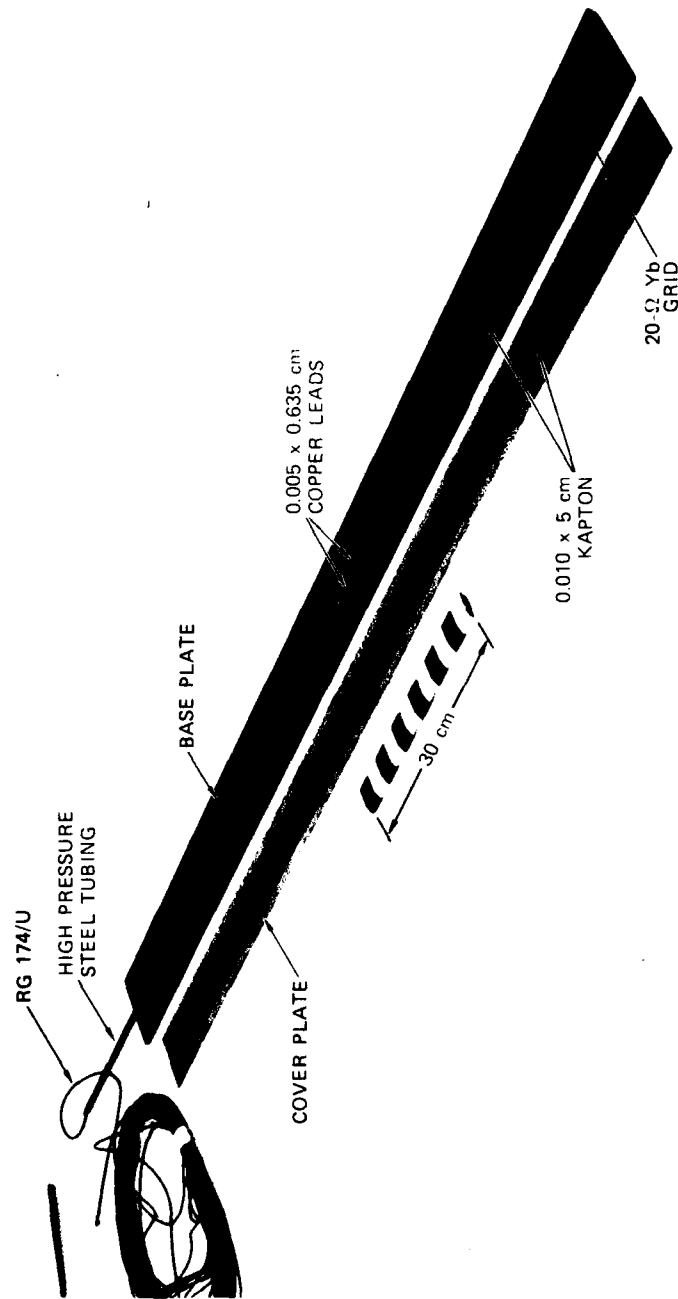
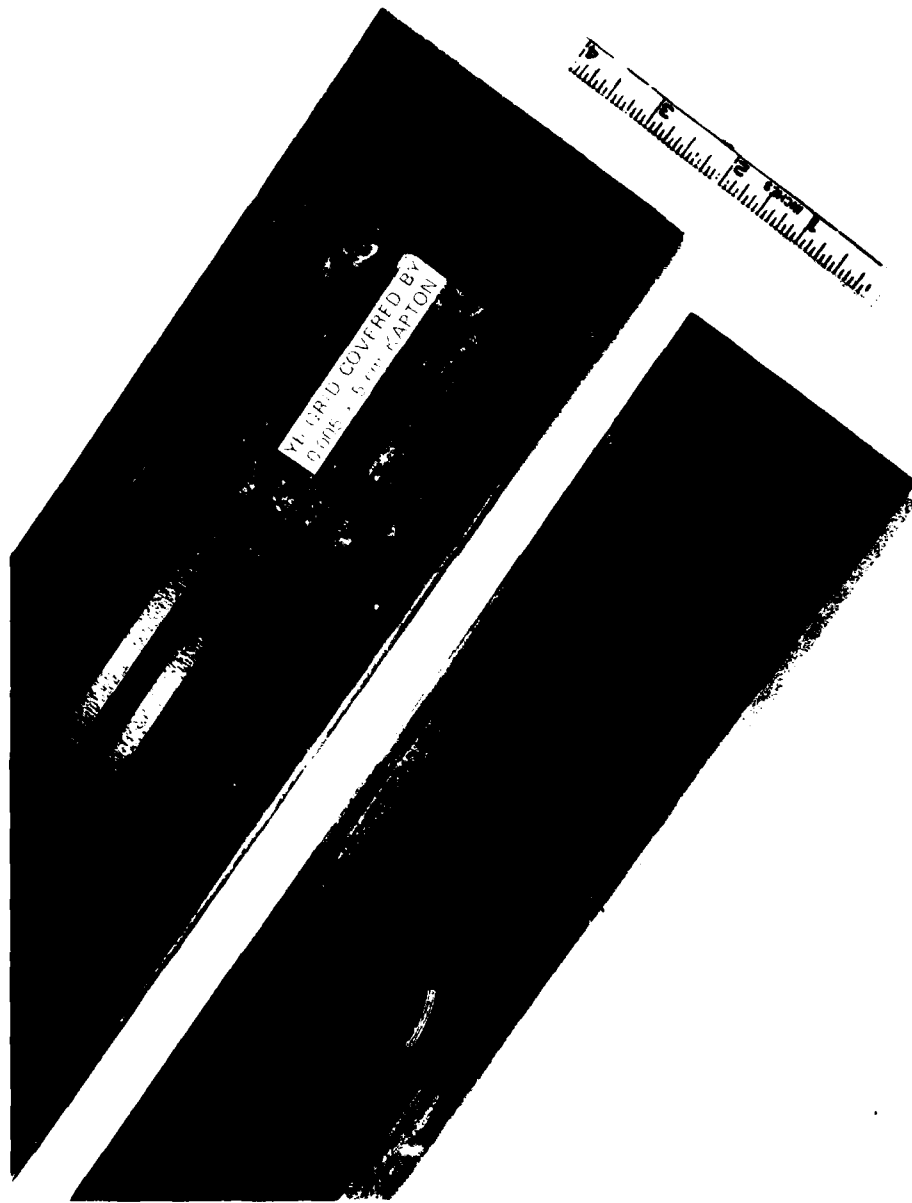


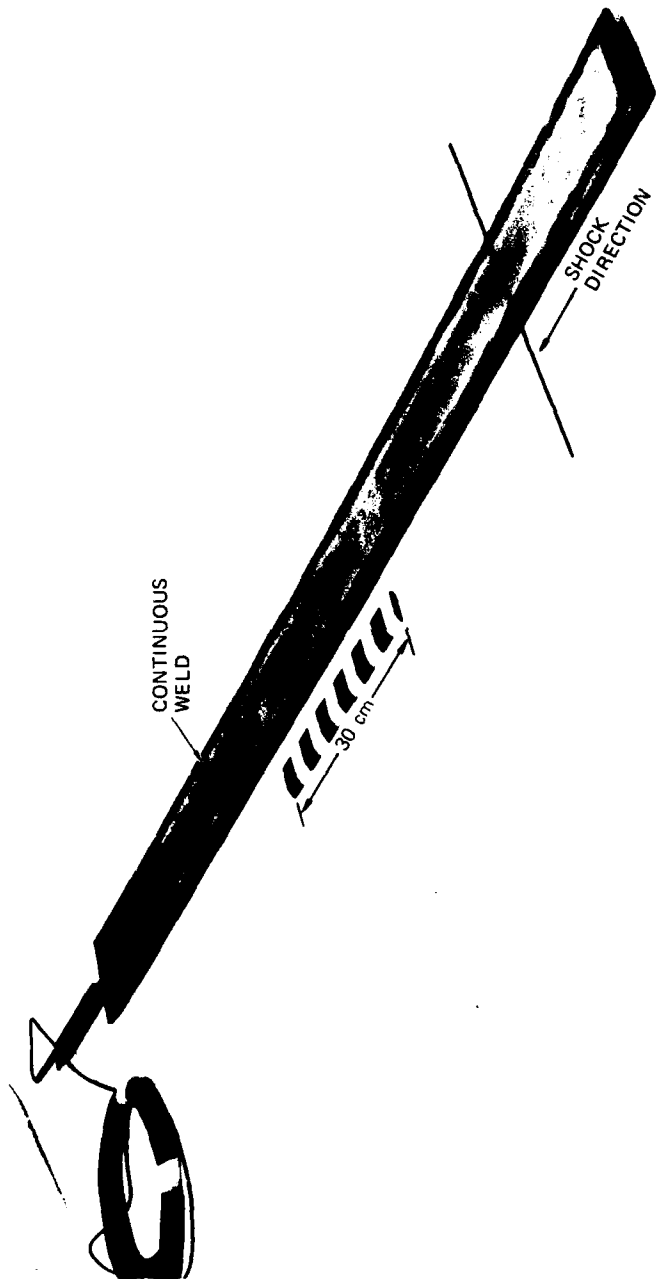
FIGURE 4 YTTERBIUM-STEEL GAGE ASSEMBLY, COVER PLATE REMOVED

MP-6334-1A



MP-6334-2A

FIGURE 5 GRID LOCATION, YTTERBIUM-STEEL GAGE



MP-6334-3A

FIGURE 6 COMPLETED GAGE ASSEMBLY

and P is the applied pressure. If we assume uniaxial strain (as indicated by our calibration tests) then, in the elastic response region, the change in thickness is:

$$(\Delta t_c)_P = P \left[\frac{t_k}{(\lambda + 2\mu)_k} + \frac{t_y}{(\lambda + 2\mu)_y} \right] \quad (2)$$

$$= \frac{P t_k}{(\lambda + 2\mu)_k} \quad \text{for } t_k \gg t_y \quad (3)$$

where k and y refer to Kapton and ytterbium, respectively, and λ and μ are the Lamé constants.

To obtain maximum thickness for the diaphragm to assure loading of the ytterbium, we arbitrarily set the deflection so that the diaphragm supports < 1% of the load, then

$$\delta_P \geq 100 (\Delta t_c)_P \quad (4)$$

For a rectangular diaphragm fixed at the edges, which approximates a worst case for our gage configuration, the diaphragm deflection is given by¹⁰

$$\delta = \alpha \frac{Pb^4}{Eh_1^3} \quad (5)$$

where α is a constant, which for our geometry and material (steel) equals 0.019, b is the smaller rectangular dimension of the diaphragm, E is Young's modulus, and h_1 its thickness. Thus the maximum thickness permissible for our arbitrary condition of equation (4) is given by;

$$h_{1_{\max}} = \left\{ \frac{\alpha b^4}{100E} \left[\frac{t_k}{(\lambda + 2\mu)_k} \right]^{-1} \right\}^{1/3} \quad (6)$$

In our configuration, $b = 7.5 \text{ cm}^2$, $E = 20 \times 10^{11} \text{ dynes/cm}^2$, $\lambda = 0.526 \times 10^{11} \text{ dynes/cm}^2$, $\mu = 0.143 \times 10^{11} \text{ dynes/cm}^2$; therefore, the diaphragm thickness h_1 must be less than 0.8 cm. In the DABS gages, this dimension was made about one-quarter this thickness, or 0.16 cm, to assure adequate response and to use readily available steel.

Since the gage is bonded to the backing plate, this plate must be rigid enough that the gage resistance change induced by bending strain is considerably less than that induced by compressive strain in the thickness direction. Acceptable minimum thickness can be found by considering Ginsberg's data² for the tensile and uniaxial strain compression sensitivities of ytterbium and estimating the tensile strain for our configuration.

Approximating the compression and tensile response of ytterbium by the linear functions,

$$\left| \frac{\Delta R}{R} \right|_B = N_1 \epsilon_B \quad (7)$$

$$\left(\frac{\Delta R}{R} \right)_C = N_2 P \quad (8)$$

where $N_1 = 3 \Omega/\Omega$; $N_2 = 3.09 \times 10^{-4} \Omega/\Omega \text{ MPa}$, R is gage resistance, ϵ is the strain, and subscripts B and C refer to bending and compression, respectively. Limiting the tensile strain signal to $\leq 1\%$ of the compressive strain signal, then

$$\left(\frac{\Delta R}{R} \right)_C = 100 \left| \frac{\Delta R}{R} \right|_B \quad (9)$$

and

$$\epsilon_B = 10^{-2} \frac{N_2}{N_1} P = KP \quad (10)$$

If we approximate the tensile strain by linear deflection of the bottom plate,

$$\epsilon_B = \frac{\Delta b}{b} = \frac{2}{b} \left(\delta^2 + \frac{b^2}{4} \right)^{1/2} - 1 \quad (11)$$

then

$$\delta = \frac{b}{2} \left[K^2 P^2 + 2KP \right]^{1/2} \quad (12)$$

From equation (5),

$$h_{2\min} = \left[\frac{\alpha P b^4}{E \delta} \right]^{1/3} \quad (13)$$

where $h_{2\min}$ is the minimum bottom plate thickness for conditions of equation (9), and therefore

$$h_{2\min} = \left(\frac{\alpha P b^4}{E} \right)^{1/3} \left[\frac{-b}{2} \left(K^2 P^2 + 2KP \right)^{1/2} \right]^{-1/3} \quad (14)$$

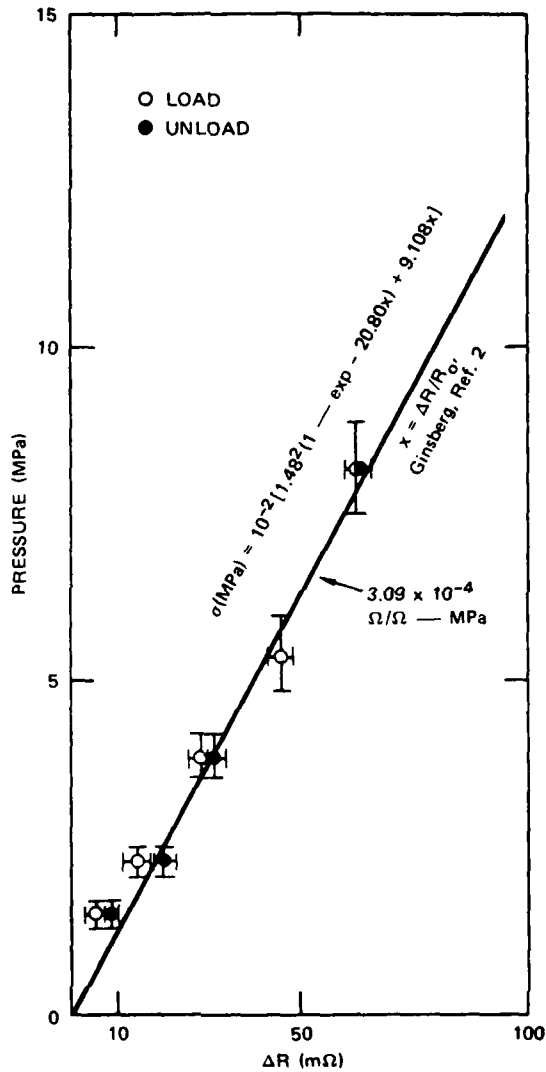
For a maximum expected pressure of 100 MPa, $h_{2\min} \geq 0.56$ cm. The bottom plate of our gage configuration was made 0.635 cm.

The rather large foil area of 5 by 7.5 cm was dictated by the need to reduce joule heating resulting from the relatively high currents (5 A) and long durations (100 ms) required to obtain adequate signal levels and long recording at the low pressures. The joule heating causes baseline drift and, if too large, can saturate the recording instrumentation. The area chosen allowed a drift of < 2 MPa ms.

Pressure calibration of the completed gage assembly was accomplished with a hydraulic press. However, three problems were encountered; uniformity of the coupling between the rams of the press and the steel casing of the gage, difficulty of measuring the actual area of coupling, and separation of pressure induced resistance changes from thermal and

tensile strain changes. To achieve uniform coupling, a high compliance material is necessary because the gage is sensitive to the tensor state of strain in the ytterbium. Rigid coupling with low compliance materials, such as steel plattens, produces bending strains in the gage package and tensile strains in the sensor, which result in an initially negative change in resistance with applied load. Best results, i.e., monotonically increasing resistance with increasing load, were obtained by using a rubber pad as the high compliance material between the upper platten and gage diaphragm. Compression and deformation of the rubber, however, caused two problems. It decreased the accuracy of measurement of the area of coupling and it permitted the platten to contact the edge welds of the gage and bridge the load applied to the diaphragm at pressures above about 8 MPa. This limited the upper range of our calibration. Although this value is below the proposed level of the DABS source, the calibration was considered adequate as discussed below. The lower limit was determined by a combination of effects; the bending strain, recording instrument resolution, and by the temperature-induced changes in the resistance of ytterbium. This limit was about 2 MPa, which represented a resistance change of 1 part in 2000. For ytterbium, this is equivalent to a temperature change of about 0.2°C or a tensile strain of $\sim 0.02\%$. For the expected lower range of the DABS environment, this pressure calibration was adequate.

The calibration obtained for the DABS configuration is shown in the pressure-resistance plot of Figure 7. Also shown is an extrapolation of the high stress, shock, one-dimensional strain data of Ginsberg et al.² for 0.005-cm-thick, unannealed foil (obtained from Research Chemical Corporation). It can be seen that the extrapolation adequately fits our static compression data for the DABS gage configuration. The error bars on the data are mainly due to the inaccuracy in determining the area over which the load was applied. The lowest data point in the shock calibration of reference 2 was ~ 500 MPa. The DABS data (see Section 4) fell within the two calibrations. Because of the good agreement between the two calibration ranges



MP-6334-4B

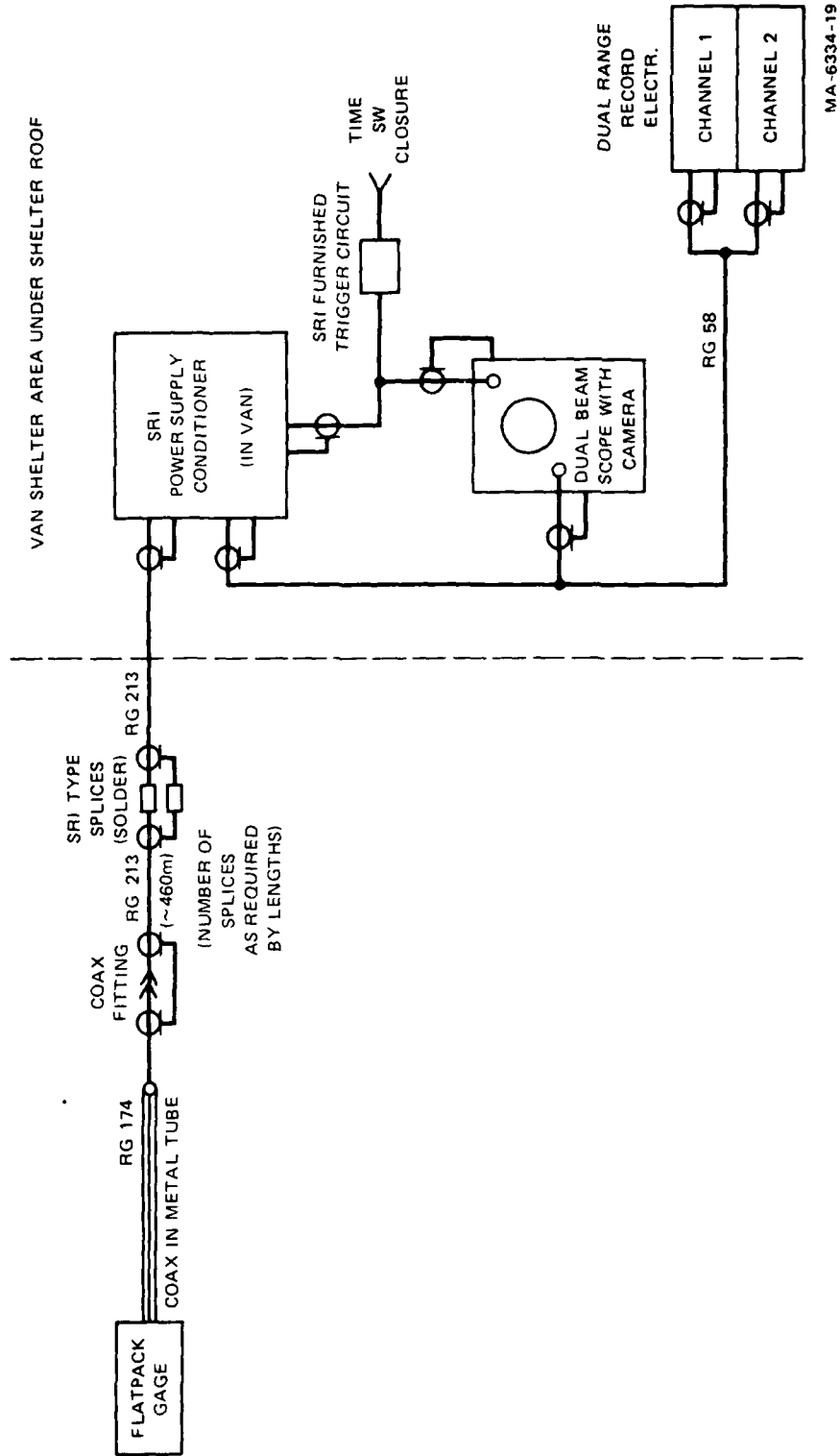
FIGURE 7 YTTERBIUM-STEEL GAGE LOAD-UNLOAD STATIC RESPONSE

and the difficulty of performing an accurate low pressure calibration on each gage, we used the one-dimensional shock calibration for the reduction of the DABS data.

Several additional aspects of our calibration are worth noting. First, the strain rate was approximately 10^1S^{-1} compared with 10^5S^{-1} for the shock loading. The response, however, is described adequately by the same piezoresistance coefficient, indicating that there are no strain rate effects. Second, the agreement between the two sets of data indicates that the precautions taken to assure one-dimensional strain compression in the steel flatpack configuration were successful and that previous low pressure static calibration data,² in which large deviations from the shock data were seen, probably resulted from ill-defined and nonuniaxial strain states in the sensor. These were probably coupled to the ytterbium from the lateral deformation of the gage packages (fiberglass or plastic) as pointed out previously.³

As can be seen from the calibration data of Figure 7, the resistance change expected in the range of 10 to 100 MPa is from 3×10^{-3} to $3 \times 10^{-2} \Omega/\Omega$ or for the 20- Ω grid, a resistance change of 0.06 to 0.6 Ω . Because of these low values, we powered the gages in a pulsed bridge supply. These supplies have been adequately described elsewhere.¹¹ To reduce ground signals between gages and recording instrumentation, the gages and coaxial shield of the cables (RG174U) were electrically floated, and both leads of the gage were insulated from the gage casing. In addition, a jointed, steel tubing system was constructed to protect the cable from the high pressure blast environment. A section of one is shown in Figure 6 at the rear of the gage. It consists of lengths of standard high pressure tube, ~ 0.635 cm O.D. by 0.16 cm wall with tapered joints. The tubing was welded at intervals to flat steel plates, which were welded to the steel floor of the DABS source chamber.

The triggering and recording system for DABS S2 is shown in Figure 8. An electrical signal was derived from the primacord HE DABS



MA-6334-19

FIGURE 8 TIMING AND RECORDING SYSTEM FOR PRESSURE GAGES, DABS S2

source initiator, shaped by an SRI pulse-shaping circuit, and then applied simultaneously to trigger the gage power supplies and recording oscilloscopes and to indicate zero time on the tape recorders.

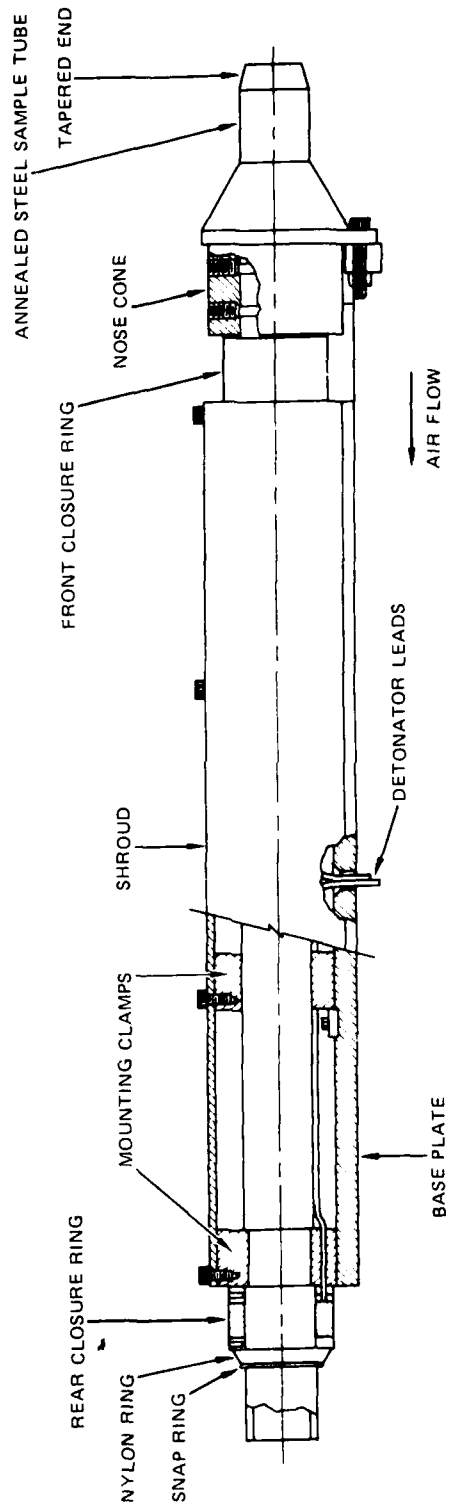
Flow Samplers

As described above, the mission of the flow samplers was to trap a volume of the flow at a prescribed time after passage of the shock front and at a fixed location along the DABS shock tube. The existing sampler design had been used at considerably lower shock pressures; therefore, the major effort of the present program was to identify and redesign portions felt inadequate for the high pressures.

We examined three areas: protection of the primacord firing system, bending of the sampler tube forward of the first explosive closure, and methods of supporting the samplers in the DABS shock tube. All three areas had been the source of failure of tubular systems in high pressure shock tube studies. The primacord vulnerability was a problem in one previous field test of similar flow samplers at lower pressure,[†] and tube bending and support structure failure occurred in air-stagnation measurements by the AFWL on DABS, S1.

In the DABS S3 tube, it was desired to sample volumes of flow \sim 10 ms and 16 ms after arrival of the shock at stations where second shocks had been observed in DABS S1. These stations were 19 and 26 m from the source array, and the expected peak pressures were about 7 MPa. It was, therefore, necessary to protect the flow samplers through a period of high pressure flow and possibly high erosion from particulate matter. This dictated that the explosive system be covered, which was acceptable for the primacord but not for the closure assemblies. A shroud over the primacord could easily contain the products from the primacord; however, a cover over the closures would result in metal fragments that might damage other instruments at these stations. A compromise was achieved by placing a shroud over the primacord only as shown in Figure 9, and using glass tape over the closure, the tape being used to protect from erosion only. In addition,

[†]W. Wilkinson, "Sampling of Dust Lofted by Air Blast Waves, Dust Sampling on Middle Gust II. Final Report, Stanford Research Institute, Menlo Park, CA (May 1972).



MA-6334-13

FIGURE 9 DABS FLOW SAMPLER

the metal parts used in prior designs of the HE closure portions were changed to plastic to reduce the threat of metal fragments. The final configuration of this HE closure ring assembly (minus the tape) is shown in Figure 10. It consists of a thimble-shaped collar around which sheet explosive (0.05 cm thick EL506 D) is wrapped (not shown) and detonated from one edge (0.48-cm hole shown in the end view) by a cap and primacord. Preshot tests of this modification showed that complete closure was obtained without rupture or fracture of the tube as shown in Figure 11. This type of sealing results if a buffer such as the plastic thimble is used between the explosive and the pipe.

To stiffen the upstream extension of the flow sampler, we added a tapered collar (Figure 8). This was locked in place by screws and a keyway in the sampler tube. In addition, provision was made for bolting the collar to the mounting stand (not shown).

The stand and mounting configuration for the DABS environment were of major concern. Requirements that affected the mounting stand design were as follows:

- The samplers must measure free-field flow conditions, i.e., away from possible boundary layer disturbances that might alter the particulate matter concentration.
- The allotted location was off the axis of the shock tube, resulting in possible large lateral stresses in the support system.
- The expected pressures (external) on the shroud might be as high as 7 MPa.

To meet the free-field flow condition, the axis of the sampler had to be at least 1 m from the shock tube wall and floor. This required a substantial support system to withstand the large rotational moment and lateral force. Attempts to modify an existing pylon design used by the AFWL resulted in a structure that was too massive and expensive for the DABS test. Although considerable design effort was spent, this concept was abandoned in favor of a simpler and less expensive "pipe" support system. The final "pipe" stand is shown in Figure 12. It consists of three "A" frames supporting a steel base

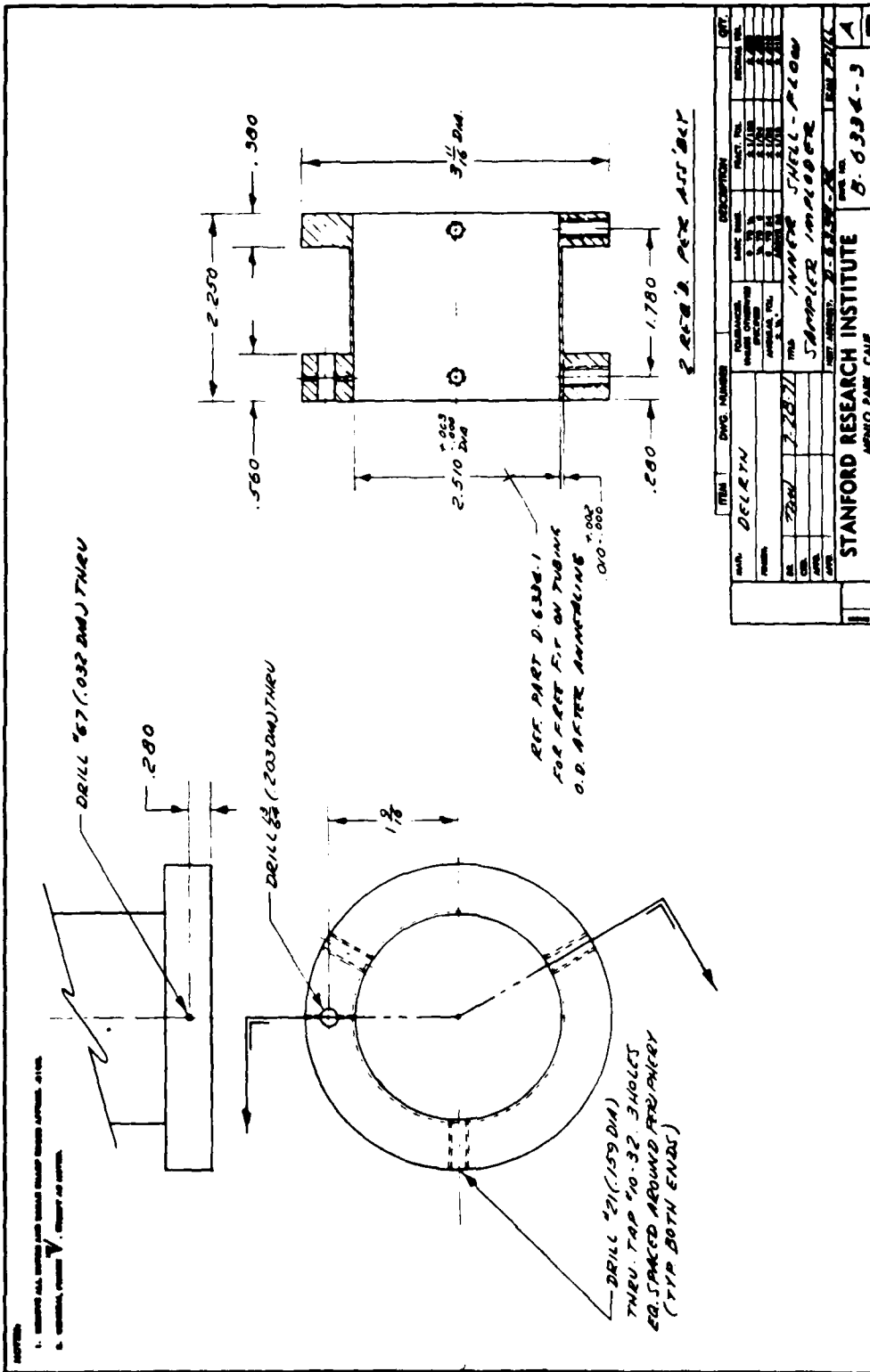


FIGURE 10 HE CLOSURE RING

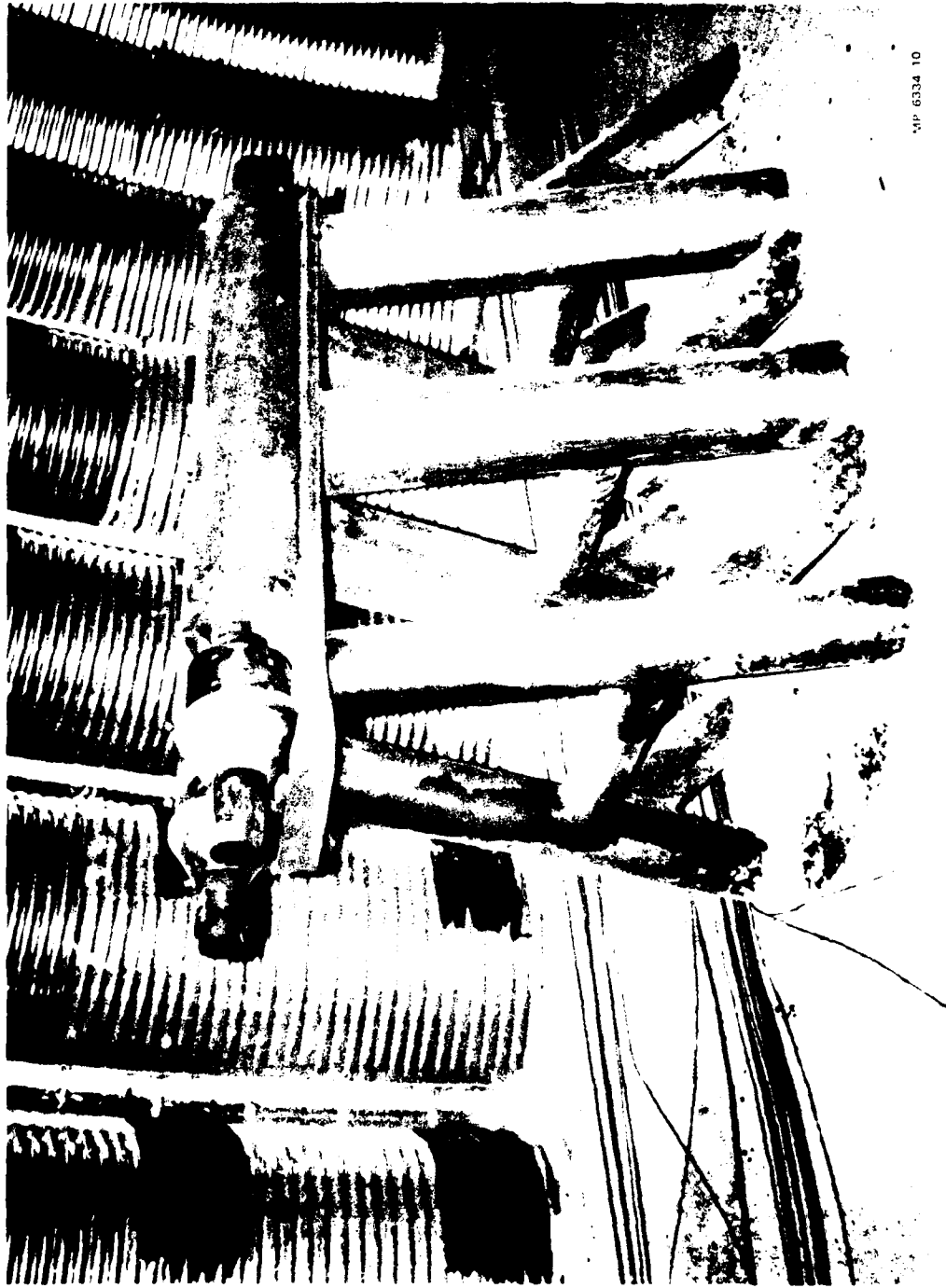


MP-6334-15

FIGURE 11 CROSS SECTIONAL VIEW OF EXPLOSIVELY CLOSED SAMPLER TUBE

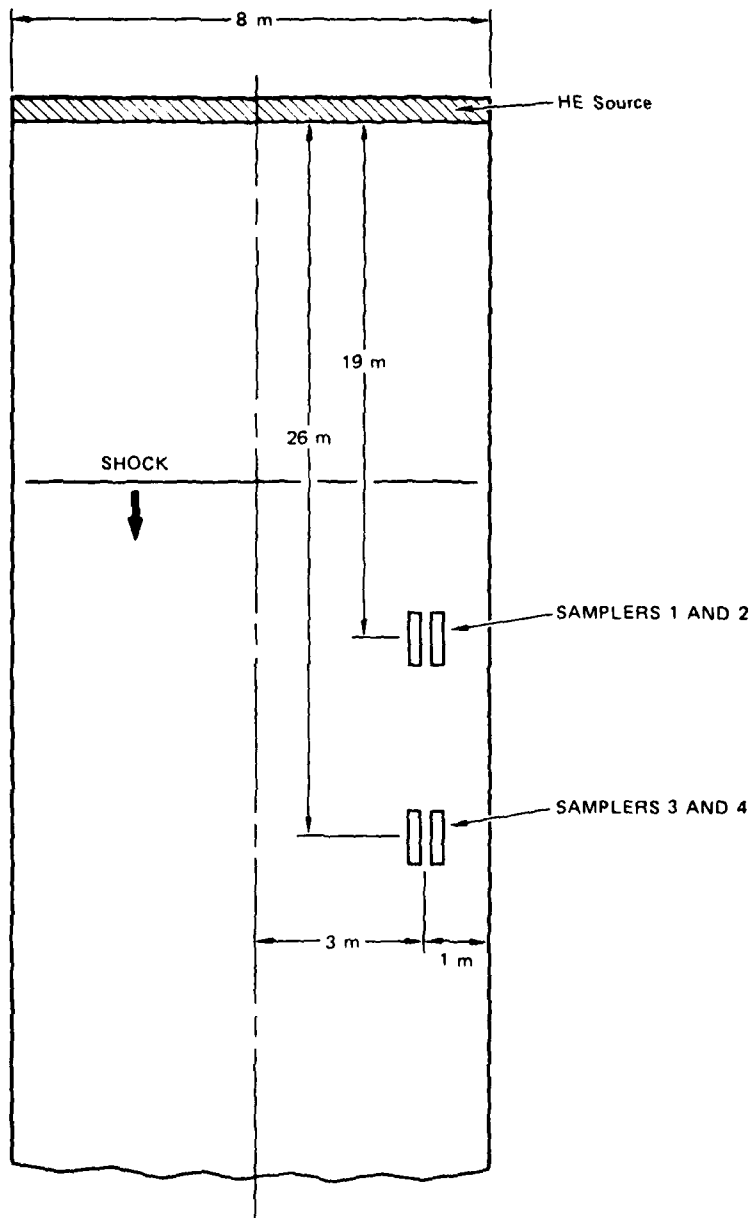
plate (1.9 by 35.6 by 96 cm) to which two flow samplers are bolted. The upstream "A" frame of each stand was constructed from 10-cm-diameter thick-walled pipes. The "A" frames are supported by angled support pipes as shown. The base of the supports are cast into a 1 by 1 by 2 m reinforced concrete base. Two stands and bases were constructed and installed by the AFWL, one at the 20-m station and one at the 28.5-m station, as shown on the plan view of Figure 13. Detonator cables were emplaced during installation of the pipe stand. The electronic detonator units (EDU) were located outside the DABS berm.

The timing and firing circuit is shown in Figure 14. A signal derived from the DABS HE source was shaped to lower its source electrical impedance, delayed by 10 and 28 ms, then used to trigger the EDUs and recorded on magnetic tape.



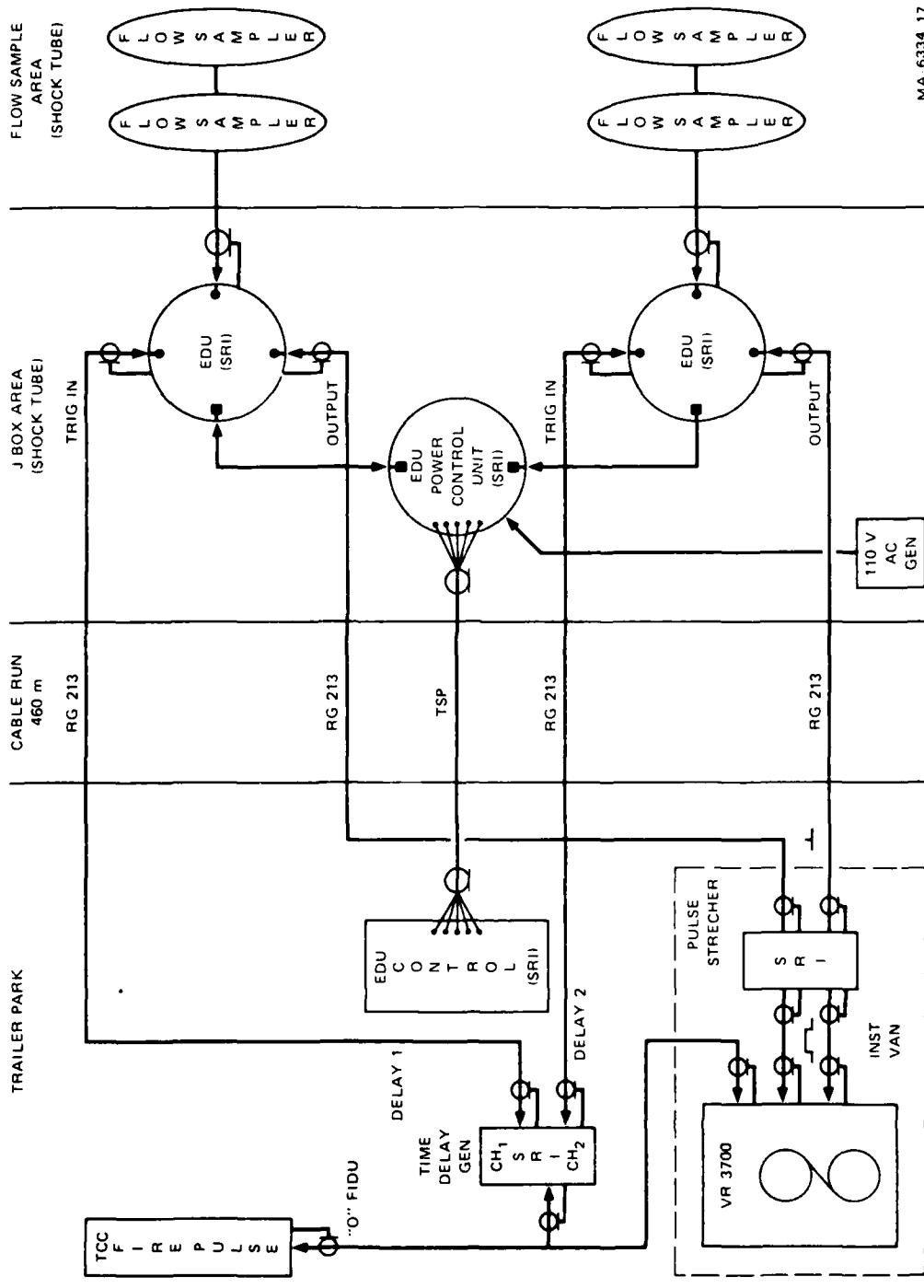
MP 6334 10

FIGURE 12 FLOW SAMPLERS, PRESHOT, SHOWING "A" FRAME STAND



MA-6334-16

FIGURE 13 PLAN VIEW OF SAMPLER LOCATION IN DABS S3



MA 6334 17

FIGURE 14 TIMING AND FIRING CIRCUITS FOR FLOW SAMPLERS, DABS S3

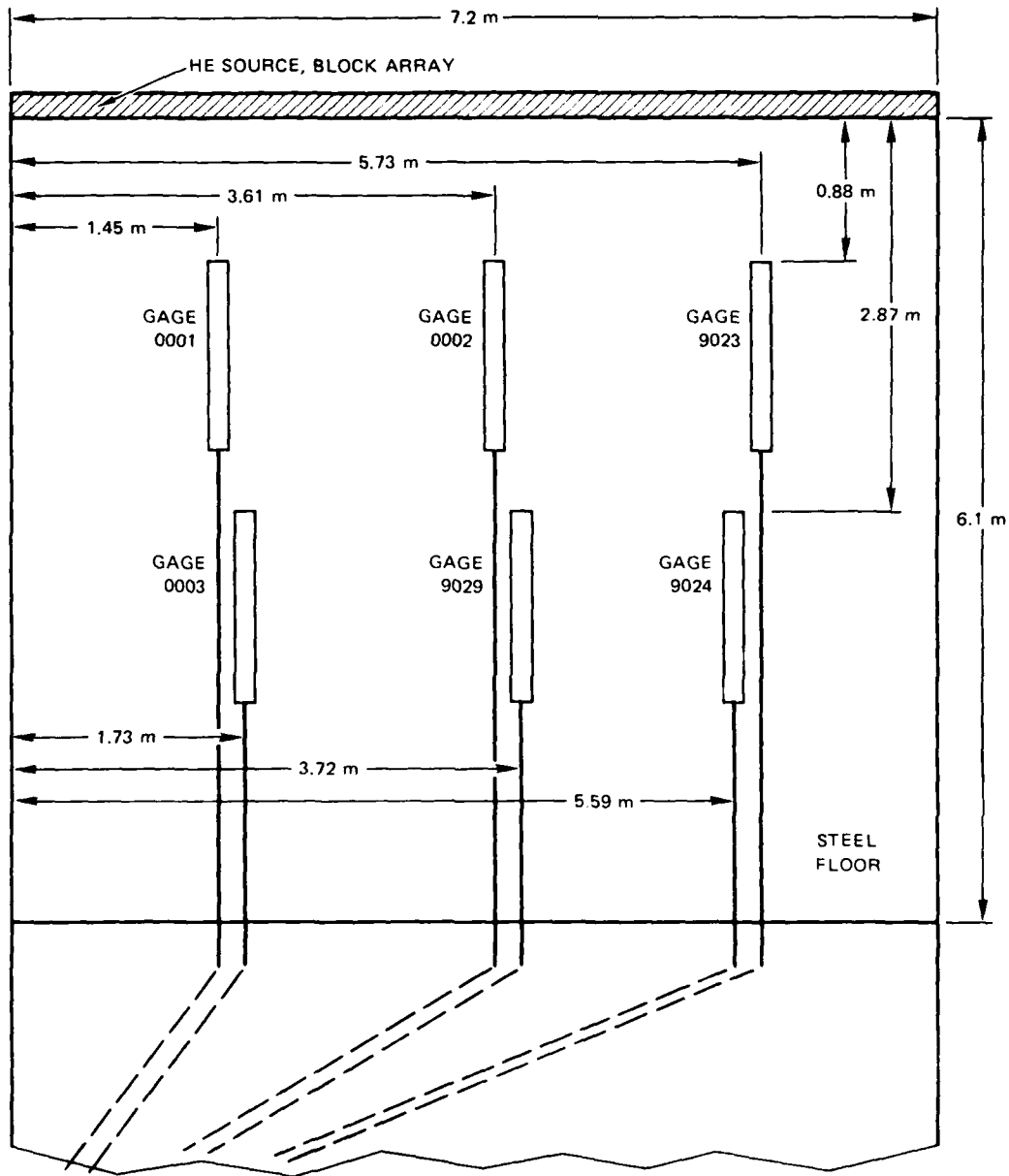
4. DABS RESULTS

DABS S2, Source Pressure

Six flatpack steel-ytterbium pressure gages were installed on the floor of the source chamber at locations shown in Figure 15. Cable protective tubing was extended to the rear of the steel flooring, at which point a transition was made to RG213U. The transition splice and cabling were buried in a 30-cm-deep trench and exited the wall of the tube beneath the edge foundations.

The cable of gage 9023 developed an electrical short between the cable shield and local ground at the source chamber after welding of the protective tube base plates to the steel floor. Because this condition violated our single point (trailer) grounding plan, we disconnected this gage and it was not used.

Pressure-time data were obtained from the five remaining gages. Reduced pressure-time traces are shown in Figures 16(a) through (e). Reduction from raw data supplied by AFWL consisted of converting voltage to pressure, defining the zero pressure voltage level, and subtracting the baseline shift. The latter two steps are necessary when using a pulsed bridge supply at high sensitivities. The deviation from electrical zero voltage was caused by minor changes in bridge balance as a result of thermally caused changes in cable resistance (~ 460 m of exposed cable). Baseline shift during the measurement was caused by joule heating of the gage and was determined before the pressure measurement. This shift was constant for each gage and power supply. Zero time in these records was taken as primacord initiation. Because the primacord was so close to the gages, it was felt that it might influence the gage readings; however, this influence appears to be minimal, as discussed below.



MA-6334-18

FIGURE 15 PLAN VIEW OF PRESSURE GAGE LAYOUT, DABS S2

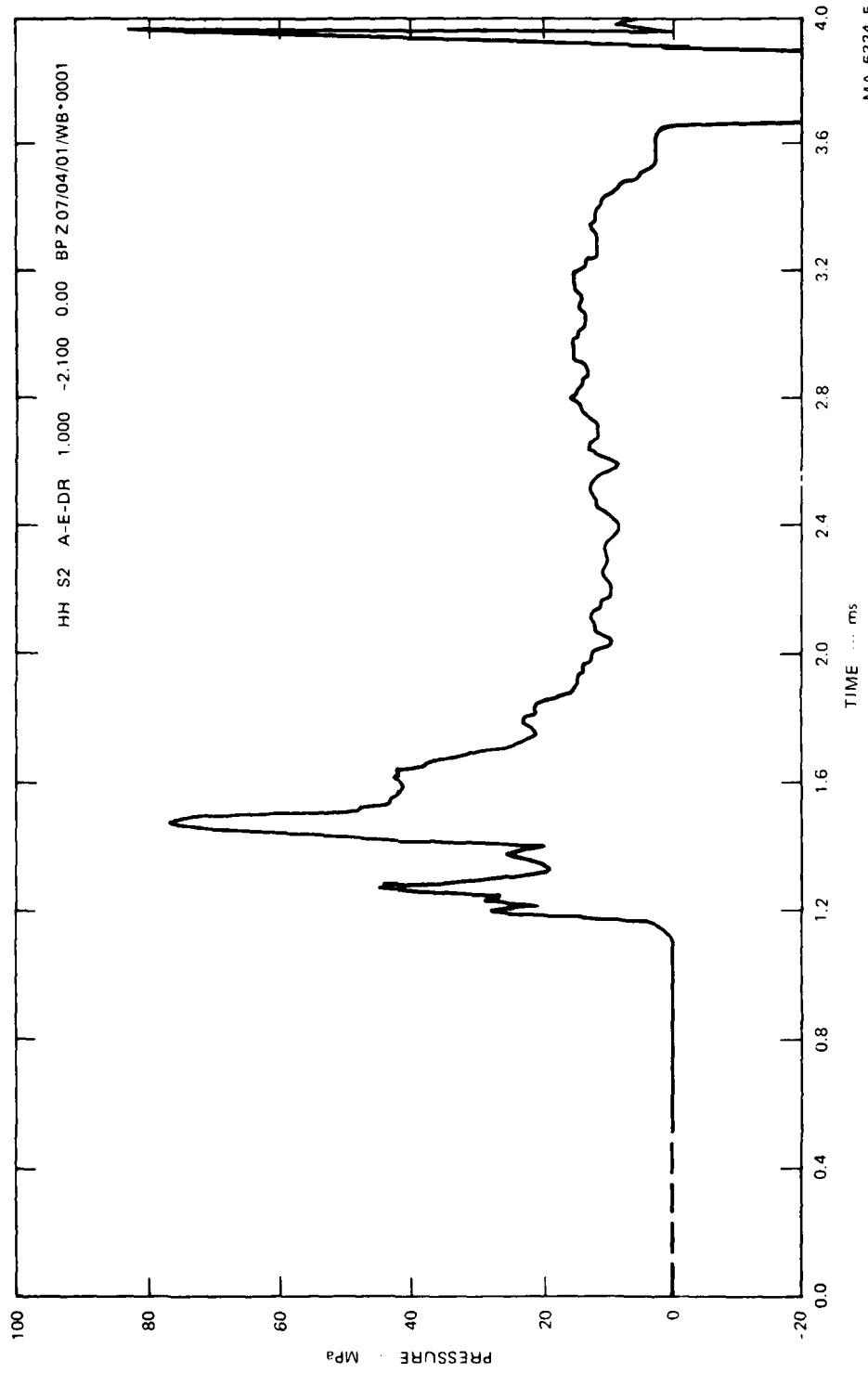
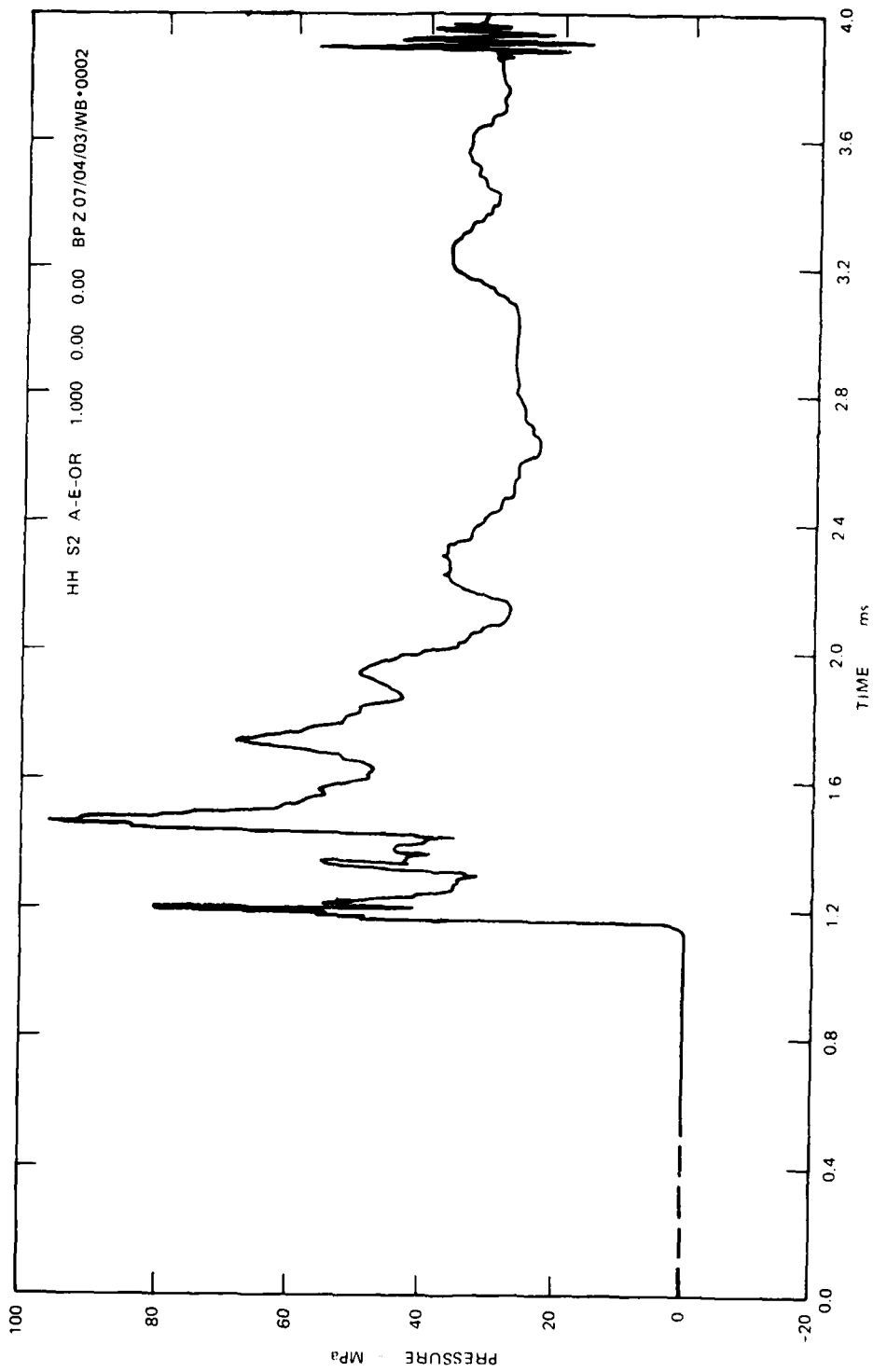


FIGURE 16 PRESSURE-TIME PROFILES. DABS S-2; GAGE 0001



MA-6334-6

FIGURE 16 PRESSURE-TIME PROFILES, DABS S-2, GAGE 0002 (Continued)

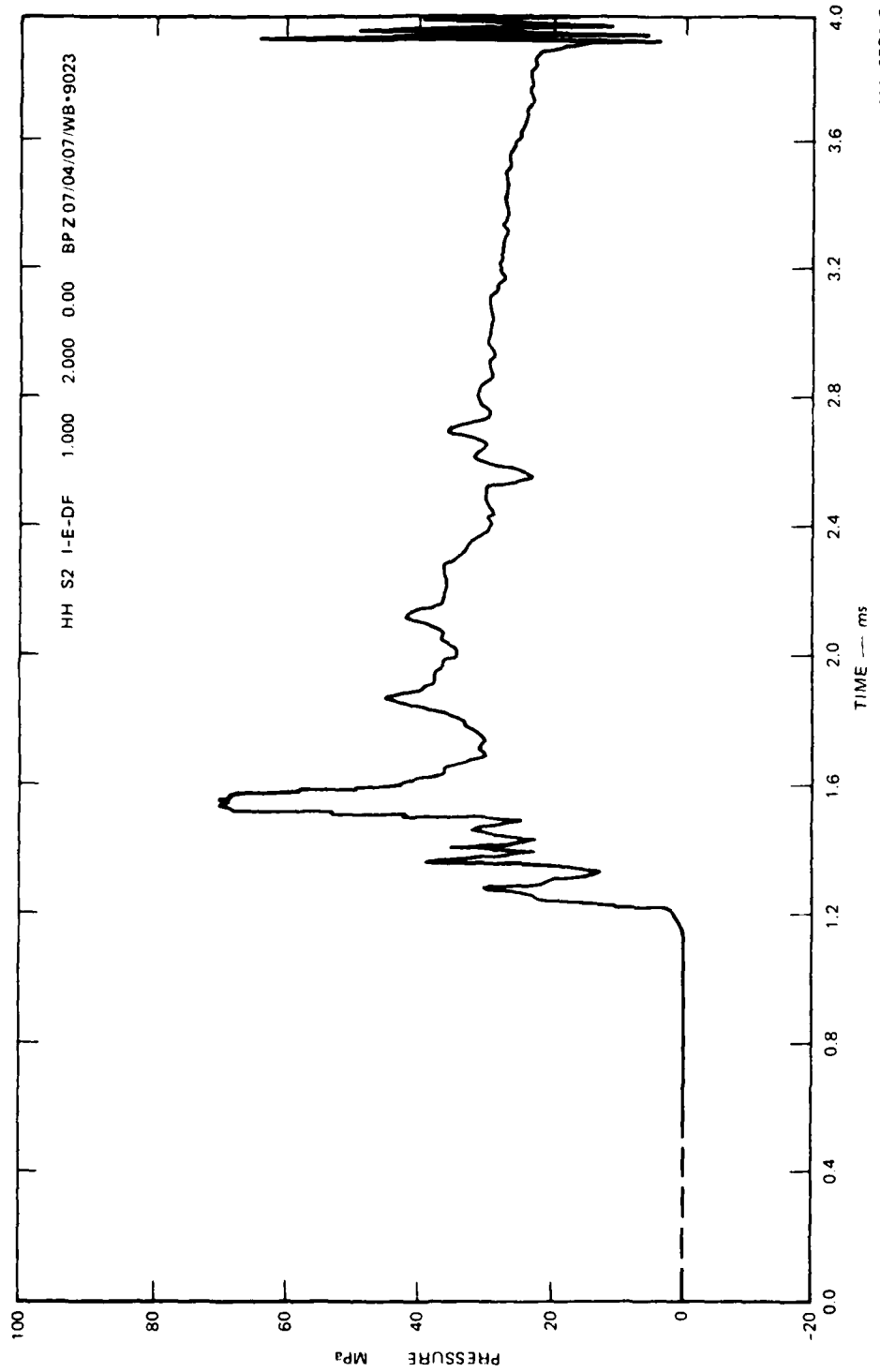


FIGURE 16 PRESSURE-TIME PROFILES, DABS S-1, GAGE 9023 (Continued)

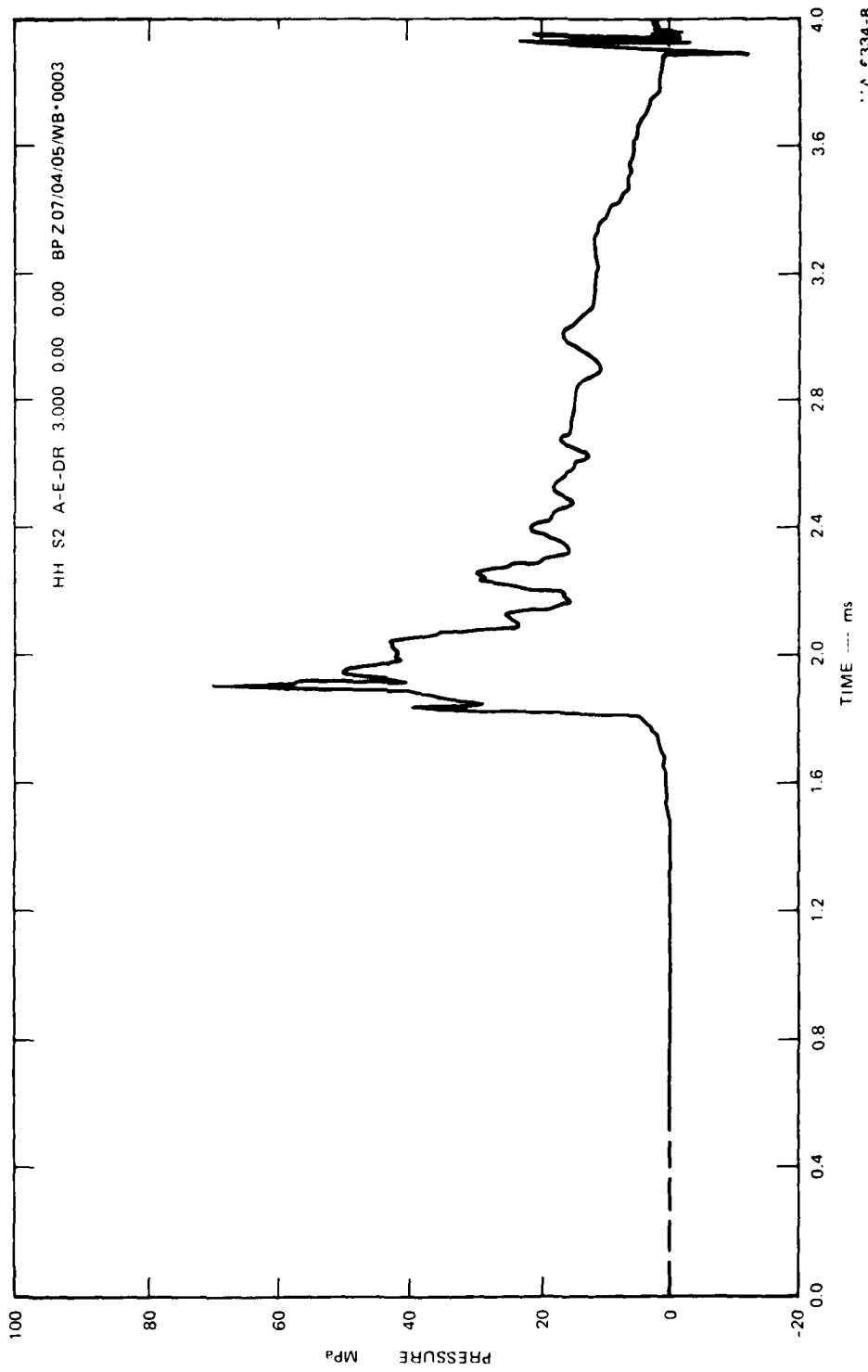


FIGURE 16 PRESSURE-TIME PROFILES, DABS S-1, GAGE 0003 (Continued)

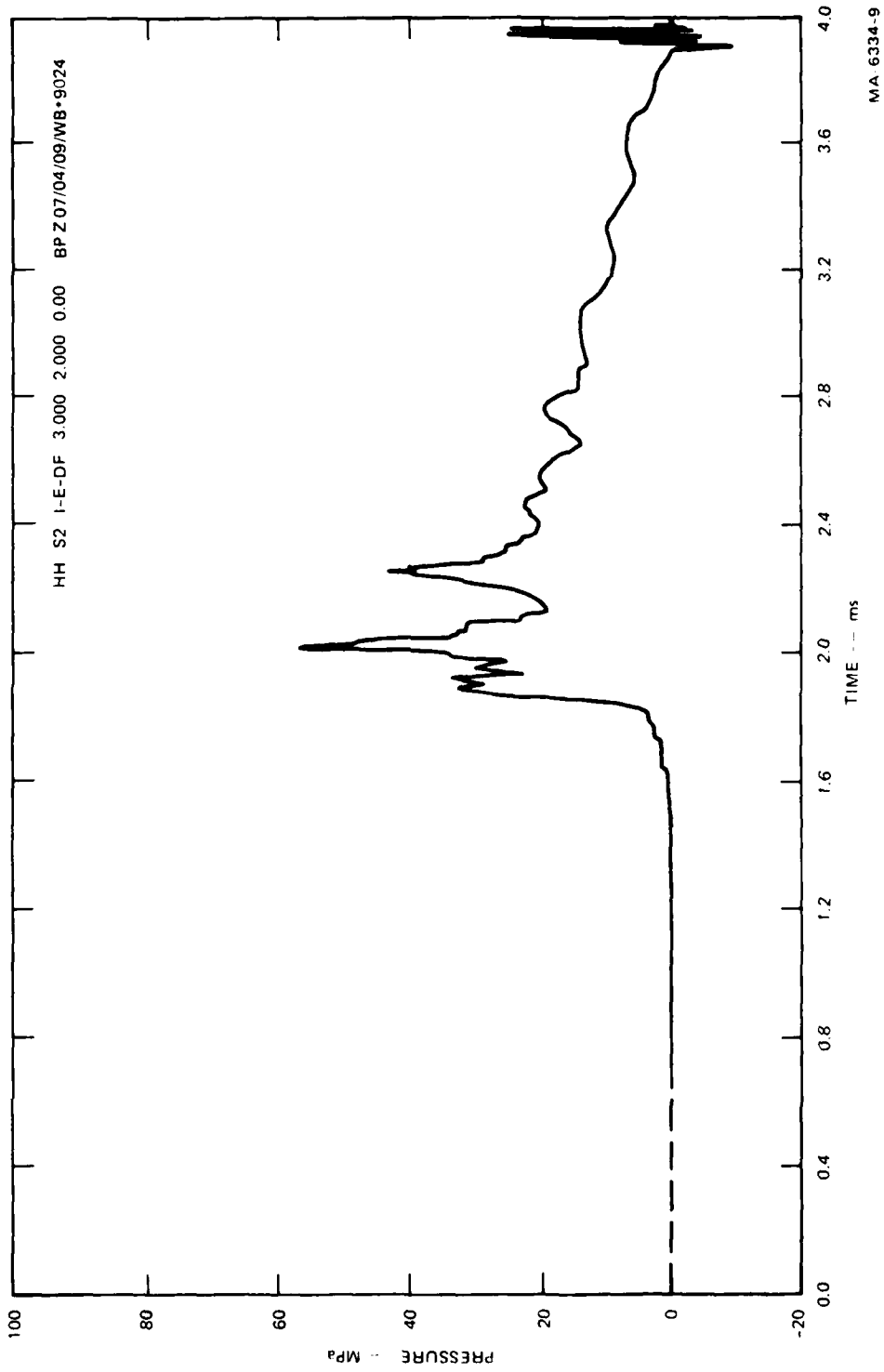


FIGURE 16 PRESSURE-TIME PROFILES, DABS S-2, GAGE 9024 (Concluded)

The general characteristics of the data are:

- An initial air shock followed by a significantly higher amplitude shock. This is most clearly seen in the records from gages 0001, 0002, and 9024.
- A periodicity to successive pressure spikes (gages 0002, 9023, and 9024).
- A prolonged positive voltage (pressure) offset at late times for the gages at 1 m (0001 and 0002), which does not occur in the 3 m gages.
- A large voltage transient on all gages approximately 3.7 m after zero time.
- Very low noise level (the low amplitude periodic nature is a result of the digital plotting routine used in reducing the data).
- Very long recording (Figure 16 shows only the initial few milliseconds; gage life extends well beyond the voltage transient).

The records were analyzed on the basis of a double shock and interpreted as an initial air shock, followed by what appears to be the contact surface between explosive gases and air. Peak pressures and velocities of the two shocks are shown in Table 1. The data are consistent; the higher shock velocities are associated with higher peak pressures. Both velocity and pressure data indicate that the pressure is higher along the center line of the chamber and that the front is slightly skewed, $\pm 5\%$. Peak pressures in the air shock range from 30 to 60 MPa, about as expected from preshot calculations (by J. Renick, AFWL, private communication).

An apparent discrepancy was found between calculated and observed velocity of the initial air shock as measured between the 1-m and 3-m gages. If we use the pressure ratio of atmospheric to the average of the first peaks together with the strong shock approximation¹² to calculate velocity, then the measured average velocity of the first wave is approximately 60% lower than calculated. However, using the same approximation, the second wave average velocity agrees to within 10% of the value calculated from the average pressure ratio, first shock to second. The most reasonable explanation for the discrepancy in the first wave is that the source chamber is prepressurized by the primacord. For the calculated velocity to agree with the observed

Table 1

SUMMARY OF GAGE DATA, SHOT S-2

Gage No.	Location (m)		Peak Pressure (MPa)		Arrival Time (ms)		Velocity (m/s x 10 ³)	
	Axial*	Transverse†	P ₁	P ₂	t ₁	t ₂	P ₁	P ₂
0001	0.88	1.45	46	76	1.18	1.42	--	--
0002	0.88	3.61	80	98	1.18	1.44		
9023	0.88	5.73	30	71	1.22	1.48	3.17	3.85
0003	2.87	3.72	40	70	1.82	1.90		
9029	2.87	1.73	-	-	--	--		
9024	2.87	5.59	34	56	1.85	2.00		

*From face of HE to front edge of Yb grid.

†From left rib, center line of gage.

first wave velocity, the "ambient" air pressure would have to be increased to only 0.5 MPa by the primacord. An approximate calculation indicates that this would require about 1.3 kg of PETN explosive, which is reasonable for the primacord.

To determine if the pressure peaks and oscillations in the profile (about a 250- μ s period) are valid, we examined possible sources of the observed profile; gage response, mounting hardware, and explosive source. The gage is essentially a piezoresistance foil bonded between a thin and a thick steel plate and backed by a thick steel plate and the ground. The fundamental resonances in the gage are the thickness and length modes of the steel plates. In the thickness mode, the time for one round-trip of an acoustic wave is about 24 μ s. Since the foil is located essentially at the air-steel interface (within 0.25 μ s), it registers the interface pressure (with the exception of a 0.25- μ s duration pulse with a period of about 2 μ s). The recorded pulse widths and periods are orders of magnitude longer than these and therefore the gage thickness resonances do not contribute to the observed profiles. The fundamental period of the floor of the chamber, (about 8 m of steel plate) is about eight times that observed in the profiles, and the period associated with the gage length is about twice that observed. The measured wave structure, therefore, represents fluctuations in air pressure and is probably due to successive shocks from various regions of the source. (The frequency is too high for lateral oscillations in the shock tube, one period at the highest velocity observed, 4.35×10^3 m/s, is ~ 1400 μ s.)

The source of the pressure (voltage) offset of the 1-m gages has not been determined. It does not appear to correlate with permanent changes in gage resistance measured after the shot (discussed below). Possible sources are temperature effects and bending of the mounting plate with a resultant lateral strain in the gage element. However, we cannot assign such behavior to the 1-m gages and not to the 3-m gages. Because of the offset, any required impulse calculations should be made only for the 3-m gages.

The large voltage spike at about 3.7 ms, Figure 16(a), coincides with the arrival of the first wave at a repair splice made in the cable and protective tubing of gage 0001. The repair was made because the insulator melted before the shot, possibly as a result of some welding performed on the cable support tube or the high ambient temperature (solar) experienced by the gages. The repair consisted of replacing a section of the cable and covering the joint with an epoxy sealer. We conclude that the epoxy coupled the pressure to the cable and that the high pressure tubing is necessary at these pressures.

The general absence of high frequency noise indicates adequate electrical grounding and shielding. At higher sensitivities, however, the low frequency baseline shift would become a problem and would require an improved system for recording the gage resistance change.

Gage resolution is within a few megapascals. Gage accuracy is approximately $\pm 15\%$, with most of the uncertainty in the gage pressure coefficient of resistance.

All gages were recovered, and postshot resistance measurements were made by the AFWL. Pre- and postshot values are given in Table 2.

Table 2

COMPARISON OF PRE- AND POSTSHOT GAGE RESISTANCES

Gage No.	Peak Pressure (MPa)	Resistance (Ω)		$\Delta R(\%)$
		Preshot*	Postshot†	
0001	76	21.3	10	-53
0002	98	21.4	21.9	+ 2
0003	70	20.0	29.9	+50
9023	71	21.3	21.6	+ 1.5
9024	56	25.3	27.1	+3.2

* Measured at SRI.

† Measured at AFWL.

In two gages, the resistance change ΔR is 50% or greater, indicating major damage to the sensor or cable. In the remaining three, one of which indicated the highest recorded pressure, there was essentially no change in resistance, tending to confirm the lower pressure static calculation data, which showed no measurable hysteresis.

DABS S3, Flow Samplers

Two samplers were installed at each of the two locations in the DABS S3 shock tube. EDU-initiated signals were executed as designed at 20 ms and 28 ms and recorded on magnetic tape. The pipe stand systems survived the blast pressures as shown in Figures 17 and 18.

Of the eight closure systems (four samplers), three of the rear units functioned as expected and one rear and all front units did not function (two pinched rear closures can be seen in Figure 17). The failure of the front closures was apparently caused by flexing of the sample tubes and baseplate as the shock passed over the assembly. An analysis of the evidence leading to this conclusion is given in the Appendix.

Although the samplers did not trap the volume of particulates representative of a specific region of the flow, it was felt that useful data might be obtained by comparing the particulate matter caught by the samplers that partially functioned with matter in the one sampler that did not function. Therefore, all four samplers were capped at the DABS site and returned to SRI. A visual inspection and sieve analysis of the contents were performed with the following results.

Samplers 1 and 2, 19-m Station, Rear Closures Functioned. The particle size distribution of the material collected in Samplers 1 and 2 was very similar. Figure 19 shows the distributions. A large fraction (10%) of very large gravel (0.5 to 1 cm) was observed. Some fragments of charred wood chips were found in the fractions from 0.04 to 0.2 cm diameter. A small amount of what appears to be soot or

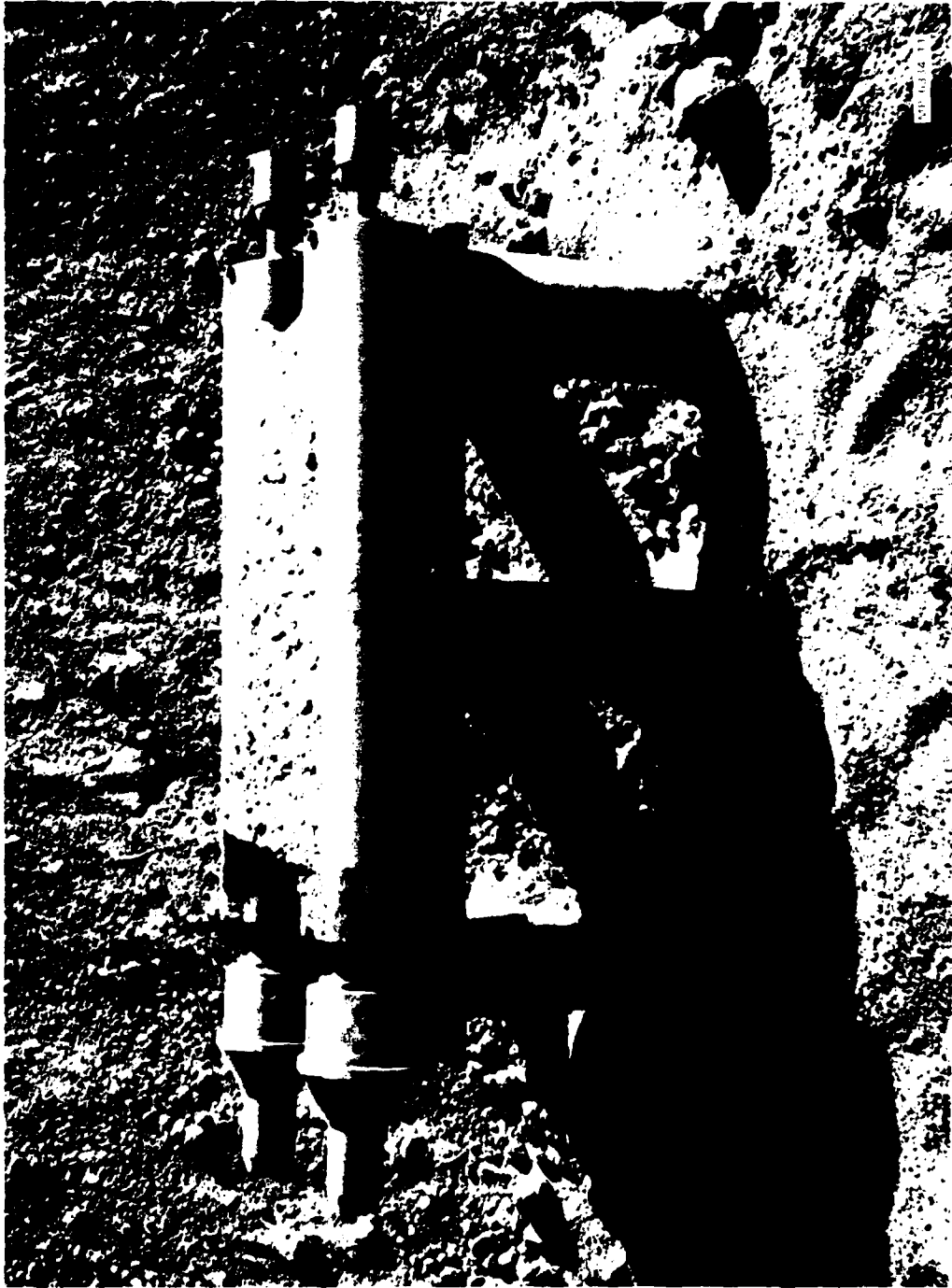
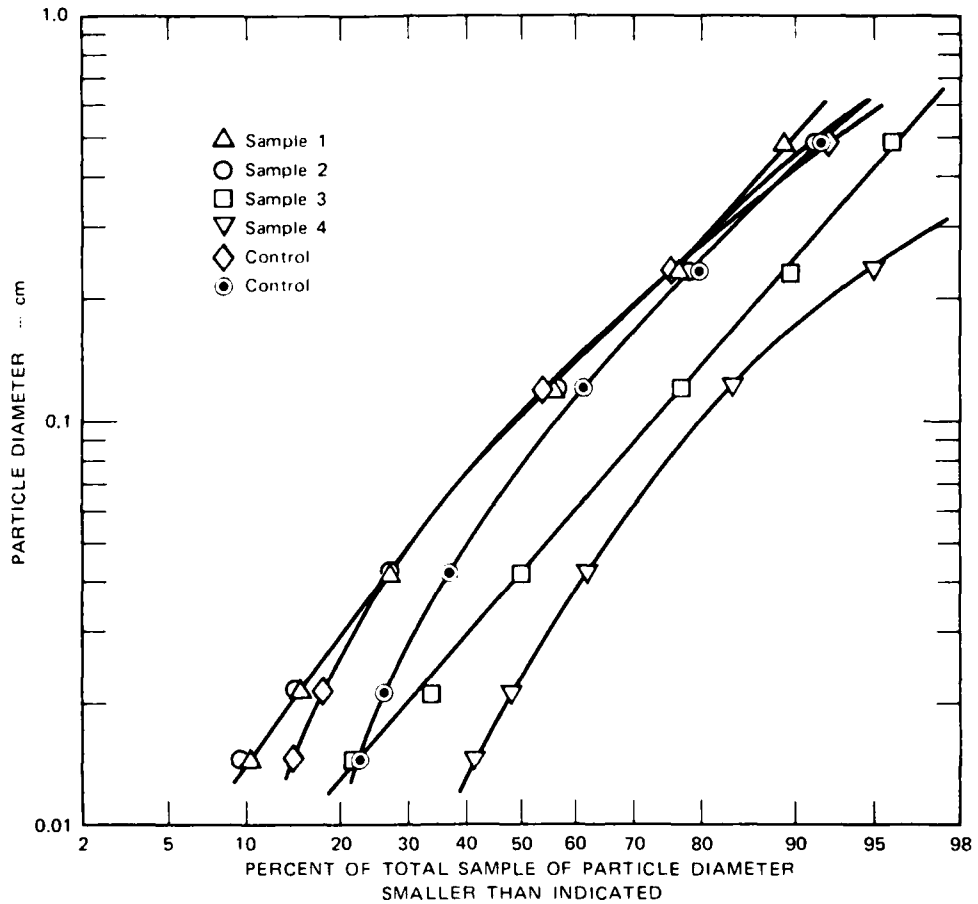


FIGURE 17 FLOW SAMPLERS (1 AND 2) POSTSHOT, STATION 19, SHOWING REAR CLOSURE (PINCHED PORTION) AND APPARENTLY UNDAMAGED STAND



MP-6334-20

FIGURE 18 FLOW SAMPLERS (3 AND 4), POSTSHOT, STATION 26, SHOWING ONE REAR CLOSURE



MA-6334-21

FIGURE 19 PARTICLE SIZE DISTRIBUTION OF FLOW SAMPLES 1, 2, 3, 4, AND CONTROL

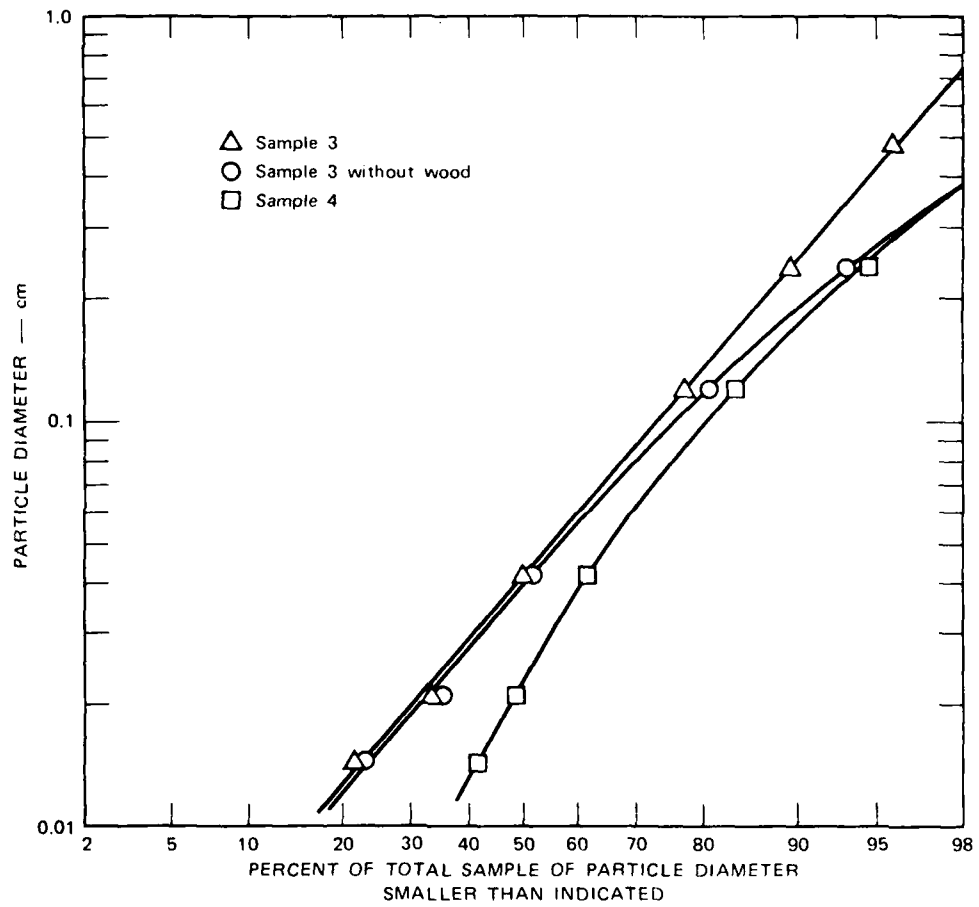
carbon particles was found in the fractions below 0.04 cm diameter. The total mass in sample 1 was 249 g; sample 2 was 293 g.

Sampler 3, 26-m Station, Rear Closure Functioned The particle size distribution of the material collected by sampler 3 indicates a higher percentage of small particles than that of samplers 1 and 2; only 4% was larger than 0.5 cm diameter. Most of the large material was wood chips. The total sample was 46.4 g.

Sampler 4, 26-m, No Closure The material in sampler 4 was very fine, no material over 0.5 cm diameter. The sampler contained very few wood or carbon particles; 78.9 g of material was collected.

Figure 19 also shows the sieve analysis of the four trapped samples and two samples of dirt collected from the vicinity of the samplers before the shot. The material collected in the upstream samplers 1 and 2 was similar to the control samples, but showed that large particles were selectively collected, which is to be expected from a closed tube in a flow field. The larger particles were able to enter the tube because of their high inertia, whereas smaller particles followed the air flow and were swept around the tube.

The material collected in the downstream samplers 3 and 4 was much finer than that collected in samplers 1 and 2, and much less material was collected. An interesting feature of these downstream samplers was the wood chips collected in sampler 3. These chips appear to be bits of particle board like that used to mount the main explosive charge. If these chips were removed from the distribution of sampler 3, the particle distribution would show a selectivity against small particles as shown in Figure 20. This would be consistent with the postulated flow around the closed tube. The smaller amount of sample collected by samplers 3 and 4 indicates that they may have been shadowed by samplers 1 and 2, which would also account for the lack of large particles in samplers 3 and 4. However, we do not have an explanation for the wood chips found in the downstream sampler 3 but not in samplers 1 and 2.



MA-6334-22

FIGURE 20 PARTICLE SIZE DISTRIBUTION OF SAMPLES 3 AND 4

A 2-g piece of what appears to be red modeling clay was caught in the rear closure of sampler 2, indicating that it was airborne 21 m down the tube and 20 ms after the main charge detonated.

These results indicate that the air flowing down the tube behind the blast wave is heavily loaded with large-diameter soil particles traveling at high enough velocity to enter the closed end sample tubes, and that its velocity is great enough that the upstream stations shadow the following stations.

Analysis of flow sampler function during passage of the shock wave (see Appendix) indicates that the base plate should be made more resistant to bending, perhaps by stiffening in the thickness direction as with an I-beam. Also, the primacord system should be more firmly attached to the HE closure ring. Successful closure of three of the systems and survivability of the samplers and mounting stand indicate that the general design can be made to function at high pressures.

REFERENCES

1. C. W. Smith, D. E. Grady, L. Seaman, and D. F. Petersen, "Constitutive Relations from In Situ Lagrangian Measurements of Stress and Particle Velocity," Final Report, DNA 28831, Stanford Research Institute, Menlo Park, CA (1972).
2. M. J. Ginsberg, D. E. Grady, P. S. De Carli, and J. T. Rosenberg, "Effects of Stress on the Electrical Resistance of Ytterbium and Calibration of Ytterbium Stress Transducers," Final Report, DNA 3577F, Stanford Research Institute, Menlo Park, CA (1973).
3. D. D. Keough, "Development and Fabrication of Stress Gages and Power Supplies for the Mighty Epic Interface Experiment," Final Report, DNA 4236F, Stanford Research Institute, Menlo Park, CA (1976).
4. E. M. Lilley and D. R. Stephens, "Electrical Resistance of Ytterbium as a Function of Temperature and Pressure," TID-4500 (UC-4) Lawrence Livermore Laboratory, Livermore, CA (1971).
5. Y. M. Gupta and D. D. Keough, "Effect of Mechanical Deformation on Piezoresistive Transducers," Research Proposal No. PYU 78-224, SRI International, Menlo Park, CA (August 1978).
6. D. H. Glenn, "Diagnostic Techniques Improvement Program, High Explosive Development Phase," Topical Report SSS-R-72-1233, Systems, Science and Software, San Diego, CA (1972).
7. P. S. De Carli, R. T. Bly, J. T. Rosenberg, and D. D. Keough, "Stress and Ablation Measurements on Hybla Gold," Draft Final Report, Contract DNA 001-77-C-0161, SRI International, Menlo Park, CA (1978).
8. T. D. Witherly, "Instruments for Measurement of Dusty Airblast Effects in High Overpressure Regions," Final Report (for Phase V), DASA 1433, Stanford Research Institute, Menlo Park, CA (1963).

9. A. R. Kriebel, "Design and Calibration of a Total-Pressure Probe for Dust-Laden Air," Final Report DASA 1158, Stanford Research Institute, Menlo Park, CA (1959).
10. R. J. Roark, Formulas for Stress and Strain (McGraw-Hill Book Company, New York, 1965), p. 227.
11. D. D. Keough, "Procedure for Fabrication and Operation of Manganin Shock Pressure Transducers," Final Report No. AFWL-TR-68-57, Stanford Research Institute, Menlo Park, CA (1968).
12. A. H. Shapiro, The Dynamics and Thermodynamics of Compressible Fluid Flow, Vol. II (The Ronald Press Company, New York, 1954), p. 1002.

Appendix

CLOSURE FAILURE ANALYSIS

Although the flow samplers and support stands appeared to be undamaged, closer inspection of both revealed that considerable flexure must have occurred during passage of the shock wave. The sequence of events, as postulated from the evidence given in Table A.1, is as follows.

Arrival of the shock wave caused the baseplate to bend upward, which in turn caused the sampler tube to bend. The front clamp was then lifted out of its groove and forward against the front closure ring. When the clamp cleared its groove, the primacord hole in the clamp no longer matched the hole in the closure ring, and the primacord was torn free of the closure explosive charge. The misalignment of the holes either pulled the primacord free or held the cord immobile so that other movement of the clamp and ring pulled it free. After the wave passed the sampler, the pylon relaxed and the clamp produced similar compression at the back of the clamp groove.

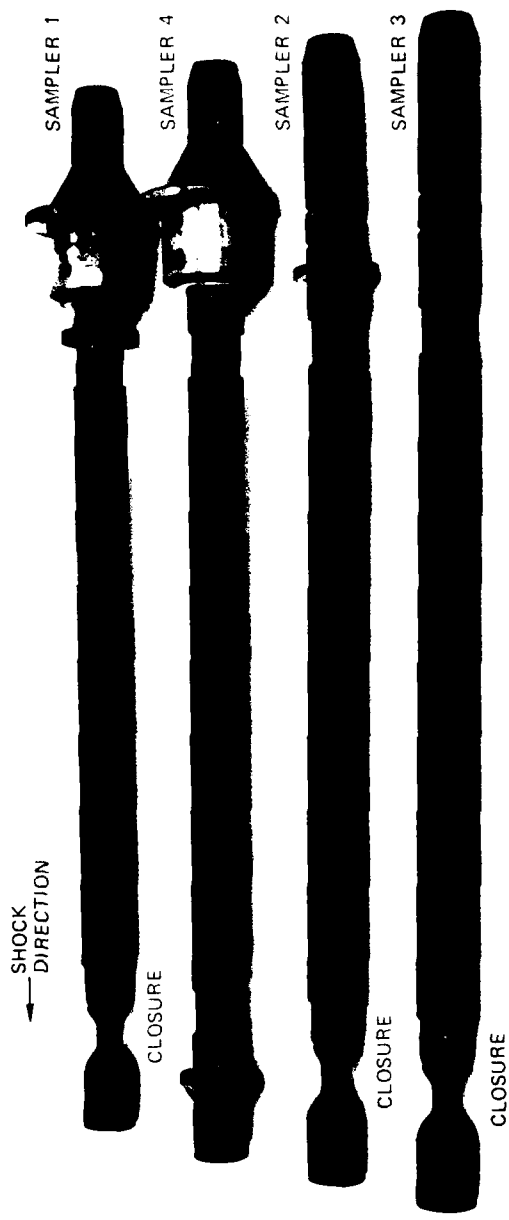
On samplers 1 and 3, the primacord was either cut or pulled completely free of the closure ring because the closure ring was intact. On samplers 2 and 4, the primacord was dislodged (but not pulled free of the closure ring) and detonated, as evidenced by missing portions of the closure rings and by carbon deposits on the remaining portions.

PRECEDING PAGE BLANK-NOT FILMED

Table A.1

SAMPLER FAILURE EVIDENCE

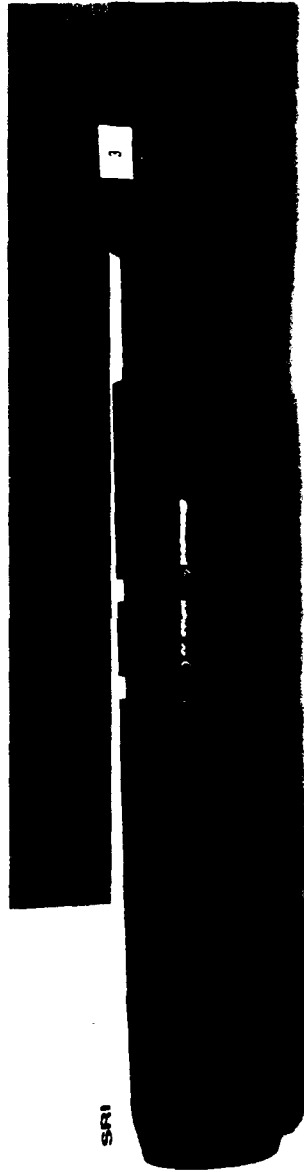
<u>Sampler No.</u>	<u>Physical Evidence</u>	<u>Figure No.</u>
1,2,3,4	Front closure failed.	A.1
4	Rear closure failed.	
3	Sampler tube bent 2°-4° at front clamp.	A.2
1	Nose cone moved backward 1/8 to 3/8 inch. All of HE closure ring remains, but compressed axially.	A.3
2	Front mounting clamp jumped forward out of its groove, compressing tube.	A.4
2	Rear mounting clamp jumped forward out of its groove, compressing tube.	A.5
4	Back closure ring with front portion missing.	A.6
2	Marks on tube indicate axial compression.	A.7



MP-6334-23

FIGURE A.1 SAMPLER TUBES, POSTSHOT

← SHOCK
DIRECTION

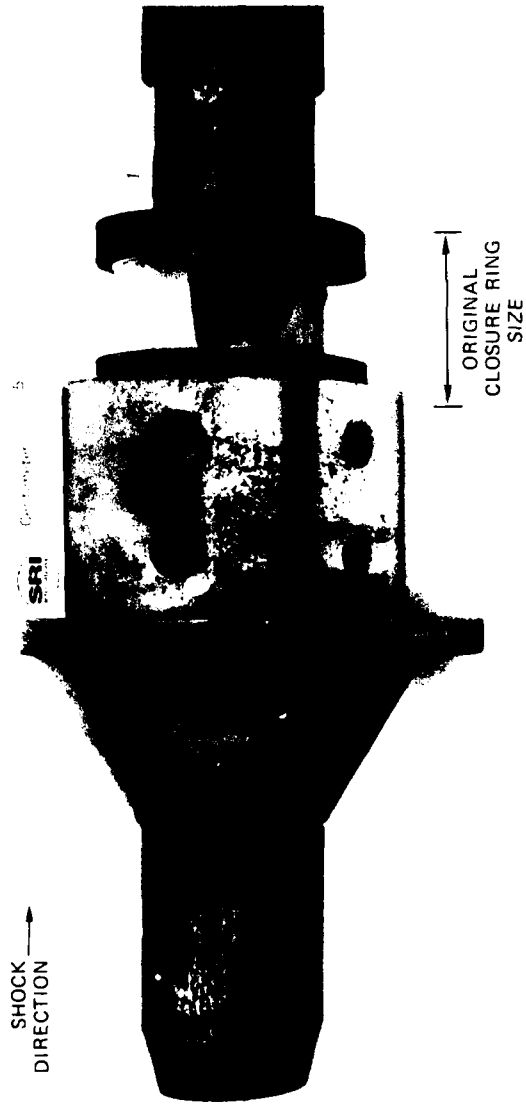


SRI

3

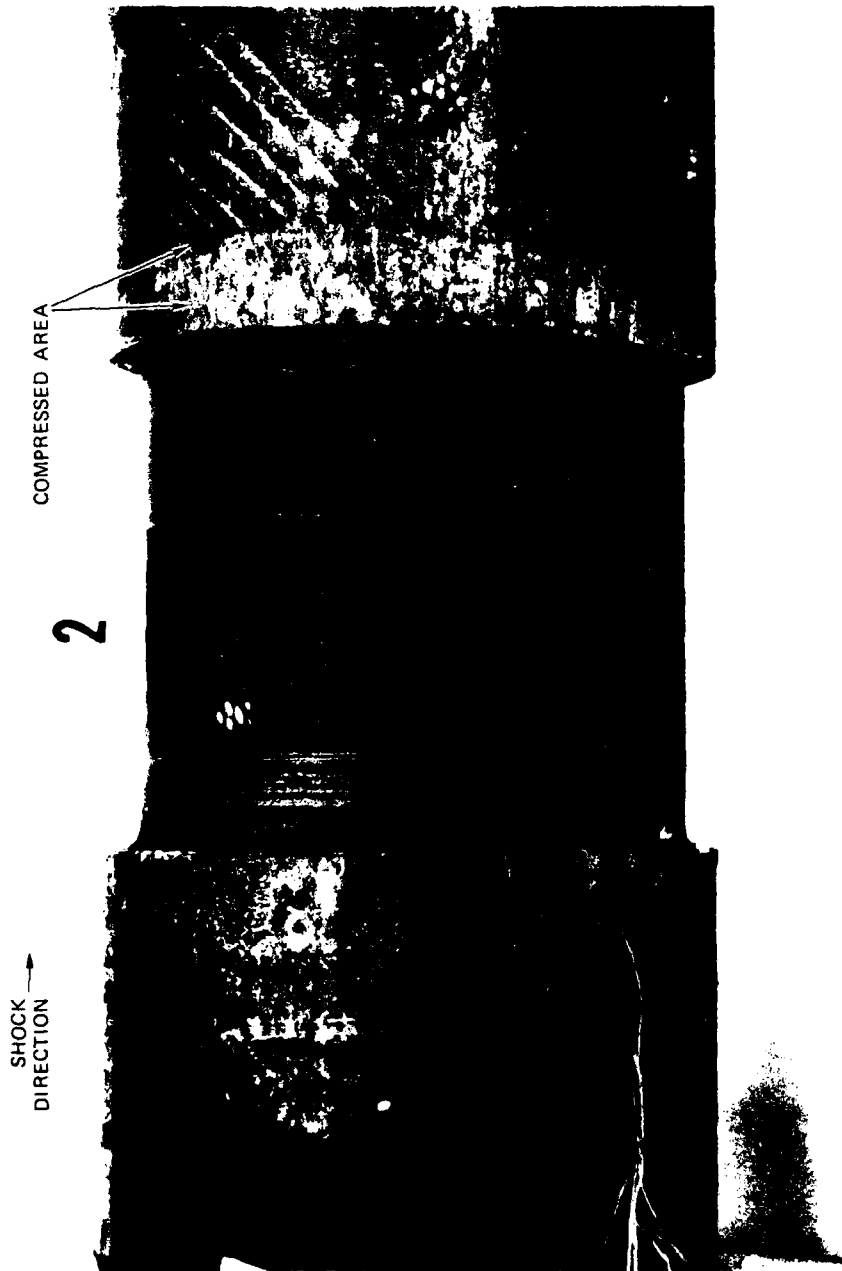
MP-6334-24

FIGURE A.2 SAMPLER TUBE 3, 2-4° BEND



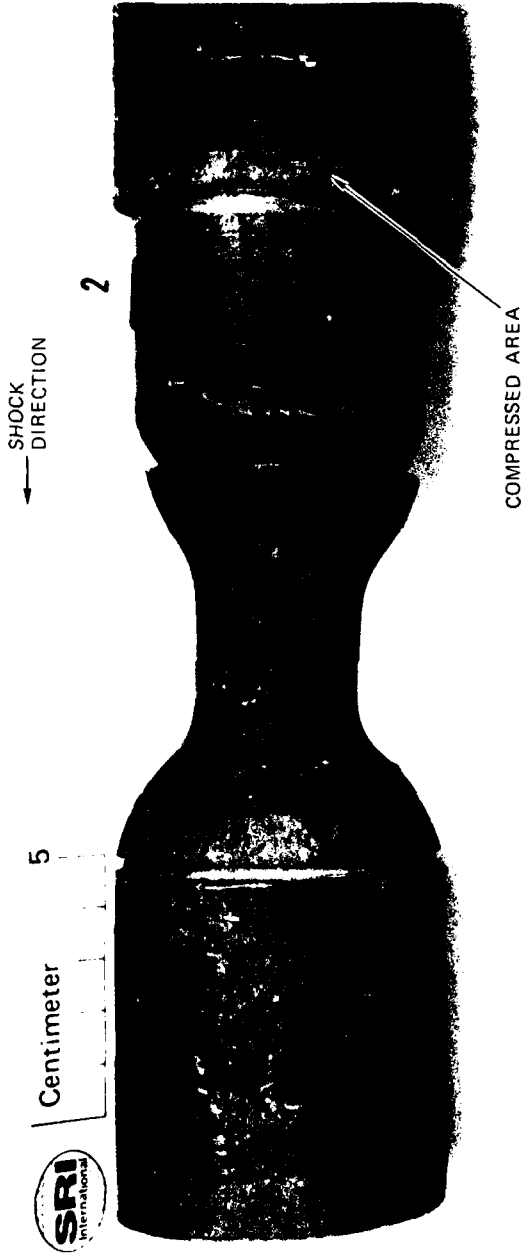
MP-6334-25

FIGURE A.3 SAMPLER 1, NOSE CONE REMOVED, HE RING COMPRESSED AXIALLY



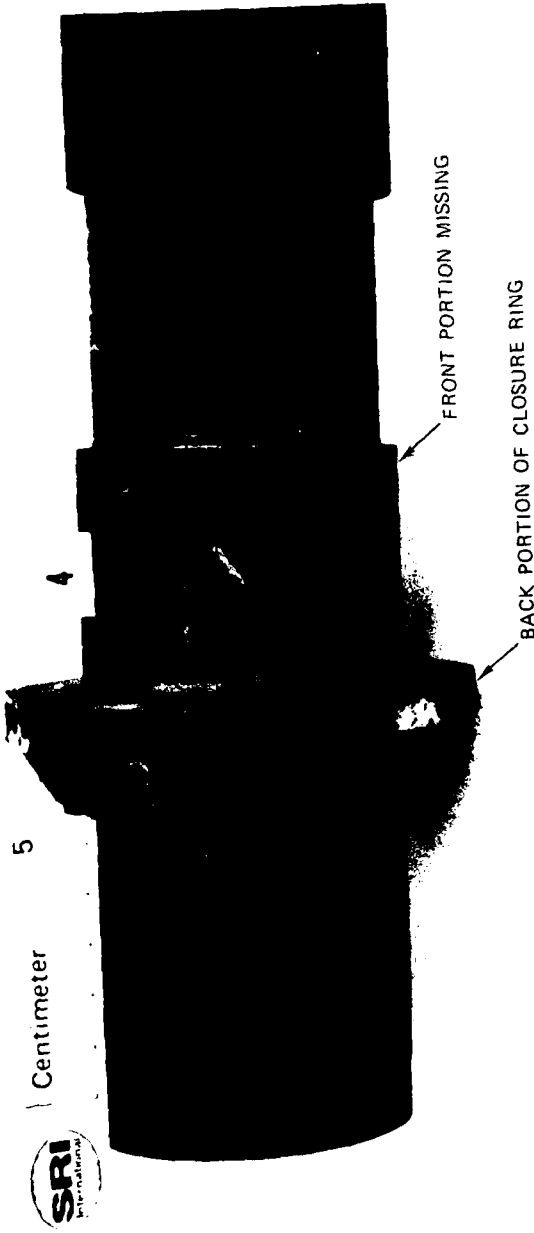
MP-6334-26

FIGURE A.4 SAMPLER TUBE 2, FRONT MOUNTING CLAMP MOVED FORWARD



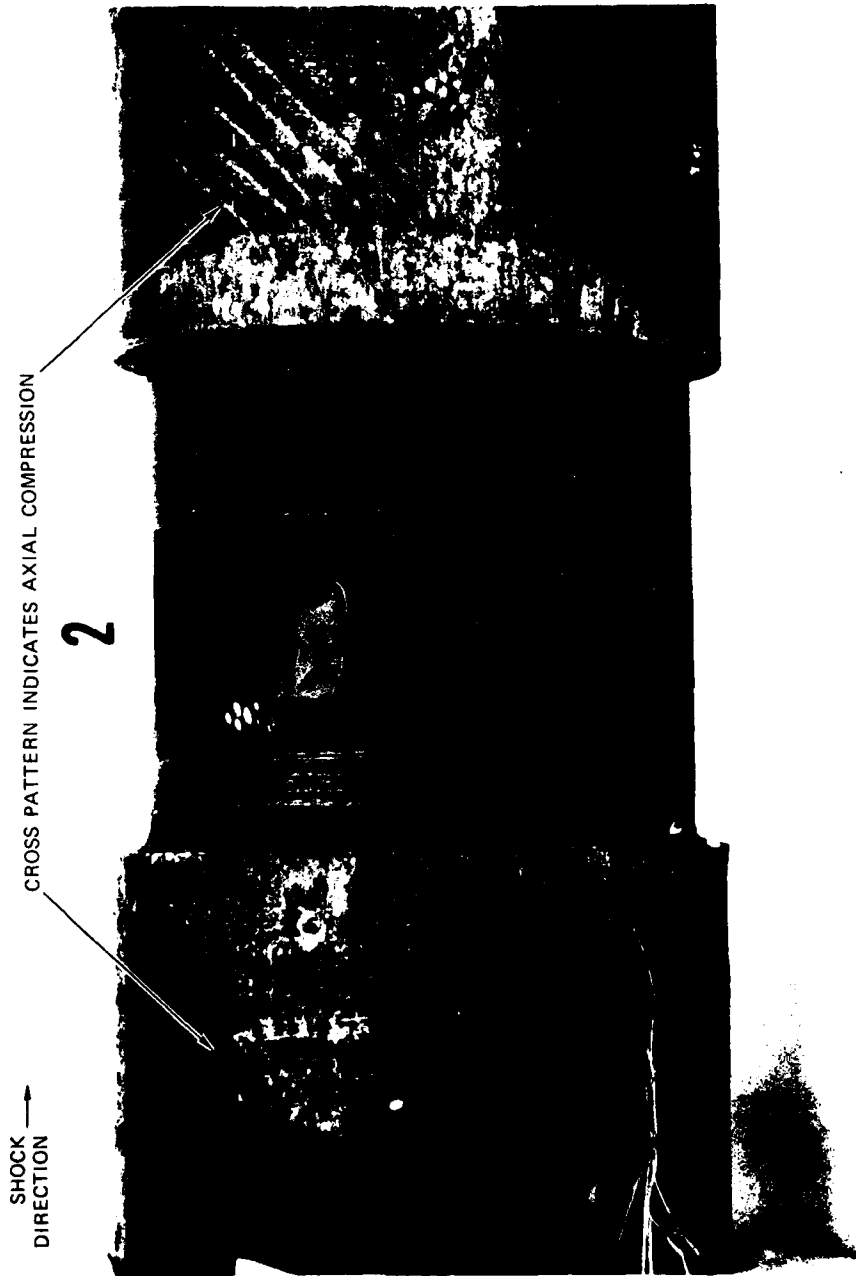
MP-6334-27

FIGURE A.5 SAMPLER TUBE 2, REAR MOUNTING CLAMP MOVED FORWARD



MP-6334-28

FIGURE A.6 SAMPLER TUBE 4, BACK CLOSURE RING



MP-6334-29

FIGURE A.7 SAMPLER TUBE 2, AXIAL COMPRESSION

DISTRIBUTION LIST

DEPARTMENT OF DEFENSE

Assistant to the Secretary of Defense
Atomic Energy
ATTN: Executive Assistant

Defense Advanced Rsch. Proj. Agency
ATTN: TIO

Defense Intelligence Agency
2 cy ATTN: DB-4N

Defense Nuclear Agency
ATTN: DDST
2 cy ATTN: SPSS
4 cy ATTN: TITL

Defense Technical Information Center
12 cy ATTN: DD

Field Command
Defense Nuclear Agency
ATTN: FCPR, J. Hill
ATTN: FCPR

Field Command
Defense Nuclear Agency
Livermore Division
ATTN: FCPRL

Joint Strat. Tgt. Planning Staff
ATTN: NRI-STINFO Library

Undersecretary of Defense for Rsch. & Engrg.
ATTN: Strategic & Space Systems (OS)

DEPARTMENT OF THE ARMY

Deputy Chief of Staff for Ops. & Plans
Department of the Army
ATTN: MOCA-ADL

Harry Diamond Laboratories
Department of the Army
ATTN: DELHD-N-P
ATTN: DELHD-I-TL

U.S. Army Ballistic Research Labs.
ATTN: DRDAR-TSB-S

U.S. Army Communications Command
ATTN: Technical Reference Division

U.S. Army Engr. Waterways Exper. Station
ATTN: Library
ATTN: WSSNS, W. Flathau

U.S. Army Material & Mechanics Rsch. Ctr.
ATTN: Technical Library

U.S. Army Materiel Dev. & Readiness Cmd.
ATTN: DRXAM-TL

U.S. Army Missile Command
ATTN: RSIC

DEPARTMENT OF THE ARMY (Continued)

U.S. Army Mobility Equip. R&D Cmd.
ATTN: DRDME-WC

U.S. Army Nuclear & Chemical Agency
ATTN: Library

DEPARTMENT OF THE NAVY

David Taylor Naval Ship R&D Ctr.
ATTN: Code L42-3
ATTN: Code 1740.5, B. Whang

Naval Construction Battalion Center
ATTN: Code LOBA

Naval Facilities Engineering Command
ATTN: Code O9M22C

Naval Research Laboratory
ATTN: Code 2627

Naval Sea Systems Command
ATTN: SEA-09G53

Naval Ship Engineering Center
ATTN: Code O9G3

Naval Surface Weapons Center
ATTN: Code F31

Naval Surface Weapons Center
ATTN: Tech. Library & Info. Services Branch

Naval Weapons Center
ATTN: Code 233

Naval Weapons Evaluation Facility
ATTN: Code 10

Office of Naval Research
ATTN: Code 715

Strategic Systems Project Office
Department of the Navy
ATTN: NSP-43

DEPARTMENT OF THE AIR FORCE

Air Force Institute of Technology
ATTN: Library

Air Force Weapons Laboratory
Air Force Systems Command
5 cy ATTN: SUL

Assistant Chief of Staff
Intelligence
Department of the Air Force
ATTN: INT

Rome Air Development Center
Air Force Systems Command
ATTN: TSLD

DEPARTMENT OF THE AIR FORCE (Continued)

Strategic Air Command
Department of the Air Force
ATTN: NRI-STINFO Library

DEPARTMENT OF ENERGY CONTRACTORS

Lawrence Livermore Laboratory
ATTN: Document Control for Technical Information Dept. Library

Sandia Laboratories
Livermore Laboratory
ATTN: Document Control for Library & Security Classification Div.

Sandia Laboratories
ATTN: Document Control for 3141

OTHER GOVERNMENT AGENCY

Federal Emergency Management Agency
ATTN: Hazard Eval. & Vul. Red. Div.,
G. Sisson

DEPARTMENT OF DEFENSE CONTRACTORS

Aerospace Corp.
ATTN: Technical Information Services

BDM Corp.
ATTN: Corporate Library

Boeing Co.
ATTN: Aerospace Library

General Electric Company-TEMPO
ATTN: DASIAC

IIT Research Institute
ATTN: Documents Library

DEPARTMENT OF DEFENSE CONTRACTORS (Continued)

Kaman Avidyne
ATTN: Library

Kaman Sciences Corp.
ATTN: Library

Merritt CASES, Inc.
ATTN: Library

Pacific-Sierra Research Corp.
ATTN: H. Brode

Physics International Co.
ATTN: Technical Library

R & D Associates
ATTN: Technical Information Center
ATTN: J. Lewis
ATTN: C. MacDonald

SRI International
ATTN: D. Keough
ATTN: L. Hall
ATTN: R. Gates

Science Applications, Inc.
ATTN: Technical Library

Systems, Science & Software, Inc.
ATTN: Library

TRW Defense & Space Sys. Group
ATTN: Technical Information Center

Weidlinger Assoc., Consulting Engineers
ATTN: M. Baron

**DATE
FILMED**

5-8